



Review

# Machine Learning Applications in the Mechanical Analysis of Nanomaterials and Nanostructures

Mostafa Sadeghian \*, Arvydas Palevicius , Paulius Griskevicius \* and Giedrius Janusas

Faculty of Mechanical Engineering and Design, Kaunas University of Technology, Studentu 56, 51424 Kaunas, Lithuania; arvydas.palevicius@ktu.lt (A.P.); giedrius.janusas@ktu.lt (G.J.)

\* Correspondence: mostafa.sadeghian@ktu.edu (M.S.); paulius.griskevicius@ktu.lt (P.G.)

## Abstract

Machine learning (ML) is increasingly used to address the computational complexity and multiscale nature of mechanical analysis in nanomaterials and nanostructures. Traditional analytical, numerical, and atomistic approaches, such as continuum mechanics, finite element methods, and molecular dynamics (MD), often suffer from high computational cost or limited scalability when applied to nanoscale systems. Recently, ML techniques have been increasingly used to predict mechanical properties, analyze static and dynamic responses, and solve governing equations of nanostructures to improve efficiency and accuracy. This review provides a comprehensive overview of ML applications in the mechanical analysis of nanomaterials and nanostructures, including mechanical property prediction, static response analysis, and vibration analysis. Various ML techniques based on the property or type of the mechanical problem are discussed in detail. The review highlights current trends and provides structured guidance for future research on reliable and physically consistent ML methods for nanoscale mechanical analysis.

**Keywords:** machine learning; mechanical analysis; nanomaterials; nanostructures

## 1. Introduction

Nanomaterials and nanostructures play an increasingly important role in modern materials engineering due to their mechanical, thermal, and multifunctional properties arising from nanoscale size effects, interfacial interactions, and complex microstructural architectures. These materials (including carbon-based nanomaterials, polymer and metal matrix nanocomposites, and architected nanosystems) are increasingly used in high-performance applications such as aerospace structures, flexible electronics, energy systems, and biomedical devices. In such applications, reliable prediction of mechanical responses including elasticity, deformation, vibration, buckling, fatigue, and fracture is essential for safe and efficient design [1–4].

In a mechanical context, a distinction is commonly made between nanomaterials and nanostructures. Nanomaterials are material systems whose internal constituents exhibit nanoscale features, including graphene, carbon nanotubes (CNTs), and nanoparticles, where mechanical behavior is mainly governed by intrinsic material properties, surface and interface effects, and nanoscale interactions. In contrast, nanostructures refer to structural components with nanoscale dimensions, such as nanobeams, nanoplates, and nanotubes, whose mechanical response is dominated by geometry, boundary conditions, and size-dependent effects [5,6]. Corresponding analyses typically focus on bending, vibration, and buckling behavior. Nanoscale structures exhibit significant size-dependent behavior,



Academic Editor: Gianluigi De Falco

Received: 24 December 2025

Revised: 7 January 2026

Accepted: 10 January 2026

Published: 15 January 2026

**Copyright:** © 2026 by the authors.

Licensee MDPI, Basel, Switzerland.

This article is an open access article distributed under the terms and

conditions of the [Creative Commons Attribution \(CC BY\) license](https://creativecommons.org/licenses/by/4.0/).

nonlocal elasticity, surface effects, and strong coupling between material architecture and structural response. These features significantly complicate classical mechanical modeling and lead to high computational costs when using finite element or MD simulations. Conventional approaches for mechanical analysis of nanostructured materials mainly rely on experimental characterization, analytical modeling, and physics-based numerical simulations. While experimental techniques provide indispensable validation, they are often expensive, time-intensive, and constrained by the difficulty of probing nanoscale phenomena. Analytical and continuum models, although computationally efficient, typically depend on simplifying assumptions that limit their accuracy for heterogeneous or highly nonlinear nanostructures. Advanced computational methods such as finite element analysis and MD simulations partially address these limitations but remain computationally demanding, particularly for multiscale systems and large parametric studies. These challenges have been widely recognized as major limitations in the mechanical design and optimization of nanomaterials [7–9].

Table 1 summarizes the classification of nanomaterials and nanostructures along with their main application areas from a mechanical perspective.

**Table 1.** Classification of nanomaterials and nanostructures and their major mechanical applications.

Category	Typical Examples	Main Applications
Nanomaterials	Graphene, CNTs, nanoparticles, polymer nanocomposites, metal matrix nanocomposites	Enhancement of elastic modulus [10], strength, fracture resistance, fatigue performance, thermal–mechanical properties [11–14]
Nanocomposite structural materials	Graphene Platelet (GPL(-reinforced composites, CNT-reinforced polymers, porous and functionally graded nanocomposites	Lightweight structural components, load-bearing applications, multifunctional materials [15,16]
Nanostructures	Nanobeams, nanoplates, nanotubes, nanorods, micro/nanoplates	Bending [17,18], vibration [19], buckling [20,21], and dynamic response of nanostructural components [22,23]
Smart and multifunctional nanostructures	Piezoelectric nanoplates, magneto-electro-elastic nanostructures, smart layered nanosystems	Active vibration control [24] and stability under multiphysics fields [25]
Architected nanosystems	Nano-lattices, hierarchical nanostructures	Energy absorption [26], mechanical metamaterials [27], stiffness and strength optimization [28]

Recently, machine learning (ML) has attracted significant attention as a data-driven modeling approach in engineering and science [29–31]. ML offers an efficient alternative by learning relationships between material, geometric, and loading parameters and the resulting mechanical responses, which enables fast and accurate prediction across wide parametric spaces. By learning nonlinear relationships directly from experimental and simulation data, ML models can predict material behavior without explicitly solving governing equations. Previous studies have shown that ML can accelerate property prediction, reduce computational cost, and enable efficient exploration of large design spaces, which is highly relevant for nanomaterials research [7,32,33].

The application of ML to nanomaterials has expanded in parallel with the growth of large-scale simulations, automated experiments, and open-access materials databases. Recent reviews show that ML has been employed across the entire range of nanomaterial analyses, including synthesis planning, structural characterization, property prediction, and performance optimization. In particular, ML methods enable the identification of

structure–property relationships that are difficult to obtain using traditional trial-and-error approaches, thereby enabling more efficient material design strategies [34,35].

Different ML algorithms has been employed in nanomaterials research (depending on data availability and modeling objectives) from classical supervised learning techniques to advanced deep learning models. Recent surveys emphasize the growing importance of graph neural networks (GNNs), which are suited for representing atomic structures and crystalline lattices as graphs, allowing direct incorporation of bonding topology and structural connectivity into predictive models [36,37].

These models are very effective for linking atomic-scale structure to effective mechanical behavior. These approaches offer clear advantages over conventional feature-based ML methods, particularly for nanoscale systems where geometric and topological information plays a critical role [36,38].

Physics-informed ML approaches have gained large amounts of attention in computational mechanics [39,40]. Reviews in computational nanomechanics report that incorporating physical laws, constitutive relationships, and boundary conditions into ML architectures significantly improves model robustness, generalization, and interpretability [37,41]. Such hybrid models provide a practical approach to connect data-driven approaches with established theories in solid mechanics, addressing one of the major criticisms of ML models with limited physical interpretability.

Despite these advances, several main challenges remain unresolved. These include limited availability of high-quality and standardized datasets, uncertainty quantification in ML predictions, lack of interpretability, and difficulties in transferring trained models across different material systems, loading conditions, or length scales. Existing review articles often focus either on general ML applications in nanomaterials or on specific material classes and optimization tasks, with comparatively less emphasis on the mechanical behavior of nanostructured materials from a unified perspective [35,37].

Motivated by this gap, the present review focuses on ML applications in the mechanical analysis of nanostructures and nanomaterials. Unlike previous studies, this work emphasizes mechanical responses (such as elasticity, bending, buckling, vibration, fatigue, and fracture) across a broad range of nanomaterial systems. This review systematically examines recent ML approaches applied to mechanical property prediction, static response analysis, and vibration analysis of nanomaterials and nanostructures. The reviewed papers cover different nanomaterials and nanostructures and include mechanical property prediction and bending, buckling, and vibration analyses.

## 2. Fundamentals of ML in Nanomaterials and Nanostructural Analysis

ML is widely used as a data-driven approach for modeling complex systems in materials science, particularly in the analysis of nanomaterials and nanostructured mechanical systems where strong size effects, nonlinearity, and multiphysics coupling limit the applicability of classical analytical approaches. In contrast to traditional physics-based models that rely on explicit governing equations, ML techniques infer complex input–output relationships directly from data, which enables efficient prediction of material behavior across high-dimensional parameter spaces [42–44].

In most nanomaterials and nanostructural studies, the application of ML follows a workflow consisting of data generation or collection, feature selection, model training, validation, and performance evaluation. Input data are commonly obtained from experimental measurements, analytical formulations, finite element simulations, or MD calculations, and may include material properties, geometric parameters, loading conditions, environmental variables, and microstructural descriptors. The outputs are usually target physical quantities of interest, such as elastic moduli, strength, vibration frequencies, buckling

loads, fracture parameters, or other mechanical responses. Most reported nanomechanical ML studies rely on supervised learning employed in mechanical analysis, where labeled datasets are available and regression models are trained to approximate nonlinear mappings between input parameters and mechanical responses. Classical ML models such as linear regression, support vector machines (SVMs), decision trees, and ensemble methods are widely used due to their robustness and interpretability. Also, deep learning architectures, including artificial neural networks (ANNs), convolutional neural networks (CNNs), GNNs, and recurrent neural networks (RNNs), are used to capture complex structural features of nanoscale systems [34,35,45,46].

To ensure reliability and generalization, trained models are typically evaluated using independent test datasets and statistical performance metrics, such as the coefficient of determination ( $R^2$ ), mean absolute error (MAE), and root mean square error (RMSE), whose mathematical formulations and parameter definitions are summarized in Table 2. In addition, the mean absolute percentage error (MAPE) is sometimes reported to provide a scale-independent accuracy indicator, particularly when comparing outputs with different magnitudes.

**Table 2.** Performance evaluation metric formulas and parameter definitions in nanomaterials and nanostructural analysis (in this table, the following parameters are defined as follows:  $y_i$ : actual value;  $\hat{y}_i$ : predicted value;  $\bar{y}$ : mean of observed values;  $n$ : number of samples).

Mathematical Formulation	Description
$R^2 = 1 - \frac{\sum_{i=1}^n (y_i - \hat{y}_i)^2}{\sum_{i=1}^n (y_i - \bar{y})^2}$	Measures goodness of fit between predicted and reference values
$MAE = \frac{1}{n} \sum_{i=1}^n  y_i - \hat{y}_i $	Average magnitude of prediction errors without considering direction
$MAPE = 100 \times \frac{1}{n} \times \sum_{i=1}^n \left  \frac{y_i - \hat{y}_i}{y_i} \right $	Relative prediction error expressed as percentage
$RMSE = \frac{1}{n} \sum_{i=1}^n [(y_i - \hat{y}_i)^2]^{1/2}$	Emphasizes larger prediction errors and reflects overall accuracy

When evaluating ML models in nanomaterials and nanostructural analysis, it is essential not only to report these metrics but also to interpret their numerical ranges and relative magnitudes in a physically meaningful manner.  $R^2$  theoretically ranges from  $-\infty$  to 1, although values between 0 and 1 are typically observed in practical regression problems. An  $R^2$  value close to 1 indicates that the model explains most of the variance in the target mechanical response, whereas values below approximately 0.8 generally indicate limited predictive capability for complex nanoscale systems, particularly when evaluated on independent test data. In vibration and stability problems, even moderate reductions in  $R^2$  may lead to significant misprediction of resonance or buckling behavior. Error-based metrics such as MAE, RMSE, and MAPE are non-negative and theoretically range from 0 to  $+\infty$ , with lower values indicating better predictive accuracy. However, their numerical interpretation strongly depends on the physical units and magnitude of the predicted quantity. For example, an RMSE value that is acceptable for predicting elastic modulus may be considered large when predicting nanoscale displacement or strain. Therefore, error metrics should always be interpreted relative to the scale of the target variable and compared across different models using the same dataset. When comparing multiple models, relative differences between MAE and RMSE are often more informative than their absolute values; a significantly higher RMSE compared to MAE may indicate sensitivity to occasional large errors [47–49].

In some studies, the MAPE is additionally reported to provide a scale-independent measure of accuracy. However, this metric can become unstable when target values approach zero and should therefore be applied with caution in nanoscale mechanical problems involving very small response values. In addition to prediction accuracy, computational cost represents an important and independent criterion for model assessment. Performance metrics such as  $R^2$  and error measures do not provide information about computational efficiency, which is instead associated with factors such as algorithmic complexity, training time, memory requirements, and hyperparameter optimization procedures. For instance, deep neural networks (DNNs) and kernel-based models may achieve high predictive accuracy but typically require greater computational resources. On the other hand, Tree-based ensemble methods or shallow neural networks often provide faster training and inference with only a small loss in accuracy. Therefore, the most suitable ML model is often one that balances predictive accuracy, robustness, and computational efficiency. Beyond data-driven approaches, recent advances emphasize physics-informed and hybrid ML methods, in which governing equations, constitutive relations, or physical constraints are embedded into the learning process. Such approaches improve model robustness, physical consistency, and extrapolation capability, which are particularly critical for nanoscale mechanical problems where data availability is often limited and experimental validation is challenging [50–53].

A conventional ANN uses a feedforward structure that takes the independent variables  $(X, T)$  as inputs, where  $X$  denotes the spatial coordinates of the problem domain and  $t$  represents time. The network outputs an approximation of the unknown physical field  $u$ , such as displacement. The predicted output  $u_{NN}$  is compared with reference data through a loss function  $L$ , typically defined using the mean squared error, and an optimization algorithm updates the network weights and biases to minimize this loss. This conventional data-driven learning strategy requires explicit training data for network calibration. In contrast to data-driven approaches, physics-informed neural networks (PINNs) do not require explicit training data. Instead, the governing differential equations and boundary conditions are directly incorporated into the loss function. The general form of the nonlinear partial differential equation considered in the PINN method is written as [54]

$$f = u_t + N[u; \lambda] = 0 \quad (1)$$

where function  $u$  should be considered in a way that  $f$  vanishes. Also, in the PINN strategy one portion of the loss function devoted to the PDE itself: [54]

$$MSE_f = \frac{1}{N_f} \sum_{m=1}^{N_f} f_{NN}^2 \quad (2)$$

where  $f_{NN}$  is the residual of the governing equation evaluated using the neural network prediction, and  $N_f$  is the number of collocation points inside the domain. The spatial and temporal derivatives required to compute  $f_{NN}$  are obtained through automatic differentiation. A second component of the loss function enforces the boundary conditions and is expressed as [54]:

$$MSE_b = \frac{1}{N_b} \sum_{m=1}^{N_b} (u_{NN} - u)^2 \quad (3)$$

where  $u_{NN}$  is the neural network prediction at the boundary points,  $u$  is the prescribed boundary value, and  $N_b$  denotes the number of boundary collocation points. The total loss function is defined as a weighted combination of  $MSE_f$  and  $MSE_b$ , ensuring simultaneous satisfaction of both the governing equations and boundary conditions during training.

A clear distinction can be made between nanomaterials and nanostructures from a mechanical analysis perspective, which is essential for selecting appropriate ML modeling strategies. Nanomaterials mainly refer to material systems in which the focus is on composition, microstructure, and nanoscale reinforcements, such as polymer nanocomposites, metal matrix nanocomposites, and carbon-based nanofillers. In this context, ML models are typically employed to predict intrinsic material-level mechanical properties, including Young's modulus ( $E$ ), ultimate tensile strength, fracture toughness, wear rate, and viscoelastic or damage-related parameters, based on descriptors such as filler content, morphology, interfacial characteristics, and processing conditions. In contrast, nanostructures emphasize the mechanical behavior of structural components with nanoscale dimensions (such as nanobeams, nanoplates, nanotubes, and architected nanoscale lattices) where geometry, boundary conditions, and loading configurations play a dominant role. ML applications in nanostructural analysis therefore focus on structural response quantities, including critical buckling loads, natural frequencies, mode shapes, deflection profiles, and dynamic response characteristics, often governed by continuum-based or nonlocal mechanical theories [55–57].

Overall, ML has become a necessary component of modern nanomaterials research, serving not only as an alternative modeling tool to reduce computational cost but also as a complementary method that enhances understanding of structure–property–performance relationships. Its integration with classical mechanics, multiscale modeling, and experimental validation provides a practical approach toward reliable, efficient, and physically consistent analysis and design of nanomaterials and nanostructured systems. Statistical performance metrics are widely reported in the reviewed literature and form the basis for quantitative comparison of different ML models in nanomechanical applications.

### 3. ML-Based Investigation of Mechanical Properties of Nanostructured Materials

Recent advances in ML have facilitated modeling of complex structure–property relationships in nanomaterials. Table 3 provides an overview of key studies using different ML approaches in nanomaterials and nanocomposites, focusing on mechanically relevant target properties, the investigated material systems, and the applied algorithms.

**Table 3.** Summary of ML techniques applied to mechanical property prediction of nanomaterials and nanocomposites.

Category	Nanomaterial/Nanocomposite	Description/Target Property	ML Model	Application Area	Ref.
Polymeric nanocomposites	Polymer–NP films	Effective mechanical descriptors	ML-based image analysis	Structural design	[58]
Piezoelectric nanocomposites	Polymer/oxide composites	Electromechanical properties	ML + phase-field	Flexible electronics	[59]
Polymeric nanocomposites	Porous heterogeneous composites	Effective mechanical properties	ML-assisted RVE	Mechanical optimization	[60]
Polymeric nanocomposites	PP-based nanocomposites	Mechanical and electromechanical behavior	ANN, GCN	Structural materials	[61]
Dielectric nanocomposites	Polymer/perovskite fillers	Breakdown strength	BPNN	Energy storage	[62]
Metal matrix nanocomposites	Graphene/Al composites	Mechanical properties	ANN, SVM	Lightweight structures	[63]
Polymeric nanocomposites	Epoxy/NP systems	Viscoelastic damage behavior	LSTM	Durability modeling	[64]

One of the main difficulties in ML for nanostructure materials is in selecting suitable algorithms for material design. Research on nanomaterials and nanotechnology often involves expensive experiments and computationally intensive analyses, which causes

increasing interest in advanced data-driven techniques such as different models of ML. These methods enable rapid extraction of relationships between the diverse structures and properties of nanomaterials. Despite the growing availability of mechanical property datasets, uncertainty often remains regarding the most appropriate learning strategy for a given material system or target response, particularly when multiple algorithms yield comparable prediction accuracy. To address this gap, quantitative structure–property relationship models have been developed using ML to select materials that meet predefined performance criteria. As reported by Jia et al. [65], ML techniques have been extensively applied to investigate defects and property variations in nanomaterials. The availability of numerous ML algorithms often creates uncertainty among researchers regarding the most appropriate method to employ for a given problem. Table 4 presents a summary of ML techniques commonly used in nanomaterials research.

**Table 4.** Summary of some ML techniques for nanostructure material investigations.

AI Algorithm(s)	Area of Application	Purpose	Reference(s)
RNNs	Discovery of new nanomaterials	Used to model how atomic clusters evolve into nanoparticles and to reconstruct structural features in thin films	[66–68]
CNN	Nanoscale structure descriptors	Applied to estimate cytotoxic effects of virtual carbon nanoparticles, identify protein-binding regions, and predict nanoparticle material properties	[69–72]
Linear regression, random forest, and deep learning	Defect analysis (surface and internal structural)	Employed to identify surface and internal defects in nanofibrous systems, microencapsulated materials, lattice structures, and polymer composites	[73,74]
Decision tree, elastic net, quadratic polynomial LASSO (QP-LASSO), and neural networks	Exploring phase-changing materials and thermoelectric materials	Utilized to screen and identify highly active materials for energy conversion and conservation applications	[75]
Deep learning	Optical properties of materials	Used to estimate refractive index of organic polymer systems based on learned structure–property relationships	[76,77]
ANN	Thermal properties of materials	Applied to predict interfacial thermal resistance in thermal interface material systems	[78]
Multiple linear regression, decision trees, k-nearest neighbor (KNN), ANN, and SVM	Electronic properties of materials	Used to predict electronic behavior and energy differences in graphene nanostructures	[79,80]
DNNs	Exploring nanomaterials with high adsorption capacity	Applied to estimate adsorption performance of nanomaterials toward organic contaminants	[81]
Random forest	Nanomaterial–biology interactions	Used to predict formation mechanisms and composition of protein coronas on nanomaterial surfaces	[82]

Jia et al. [65] reviewed how ML had been used to accelerate the design, discovery, and application of nanomaterials by replacing or complementing costly experiments and time-consuming simulations. It reported that ML models such as random forest, SVMs, ANNs, CNNs, and ensemble learning were successfully applied to predict nanomaterial structures, electronic, thermal and optical properties, adsorption and catalytic performance, and biological interactions using descriptors derived from composition, geometry, defects,

and processing conditions. The paper showed that ML achieved prediction accuracies above 90% in stability and property prediction,  $R^2$  values greater than 0.98 for defect performance relationships in metal–organic methods, relative prediction errors below 2% for electrical properties in nanocomposites, and accuracies exceeding 94% for in vivo nanoparticle accumulation and up to 98% for nanotoxicity classification. At the same time, the review emphasized that data quality, database completeness, and interpretability remain limiting factors for reliable deployment.

Several studies illustrate how ML methods are used to specific materials and mechanical outputs. Guo et al. [83] combined nanoindentation experiments, micro-area X-ray diffraction, and ML to link mineral composition with local mechanical properties in heterogeneous conglomerate rocks. Nanoindentation-based elastic modulus and hardness data were clustered using unsupervised learning (K-means and hierarchical clustering). A random forest regression model then predicted mineral composition from mechanical inputs, achieving  $R^2$  values of 0.81 for quartz and 0.85 for clay minerals, with normalized RMSE  $\approx$  0.10, demonstrating that mechanical measurements can be used as informative proxies for compositional inference in highly heterogeneous systems.

A related trend is the use of ML models to reduce experimental workload in composite design. Okasha et al. [84] predicted elastic modulus and flexural strength of CNT-reinforced cementitious composites using ANN, support vector regression (SVR), and histogram Gradient Boosting (HGB). Their dataset included 117 points for elastic modulus and 146 points for flexural strength and was split into training (60%), validation (20%), and testing (20%) subsets after preprocessing. Inputs captured mixture proportions and processing descriptors: for elastic modulus, water-to-cement ratio, sand-to-cement ratio, curing age, CNT content, and CNT surface condition were used; for flexural strength, additional parameters such as CNT aspect ratio, surfactant-to-CNT ratio, and time were included. This setup highlights a practical modeling choice in nanocomposite mechanics: property-specific inputs can be necessary because different responses depend on different physical descriptors.

Simulation-driven datasets are also widely used to train fast models for mechanical responses. Luo et al. [85] coupled molecular dynamics (MD) simulations with supervised learning to predict tensile behavior of graphene-reinforced polyethylene composites. Feed-forward neural networks (FFNNs), SVM, and Adaptive Boosting (AdaBoost) regression were trained using features including temperature, tensile strain rate, graphene volume fraction, graphene deletion rate, and polyethylene chain length, with outputs of ultimate tensile strength and elastic modulus. The FFNNs achieved  $R^2$  values above 0.99 for ultimate tensile strength and above 0.92 for elastic modulus on test data. Ultimate tensile strength increased from about 156.9 MPa to 194.3 MPa as graphene volume fraction increased from 3.4% to 5.7%, and a graphene deletion rate of 7.9% improved tensile strength by about 29.4% compared to pristine graphene, indicating that ML models can capture coupled processing/structure effects learned from atomistic data while enabling rapid evaluation across parameter space.

At the atomistic scale, ML has also been used to replace expensive ab initio calculations with learned interatomic potentials. Hawthorne et al. [38] developed an ML interatomic potential for graphene based on the Deep Potential method, trained on density functional theory data with atomic environment descriptors as inputs and atomic energies as outputs (forces and stresses derived via automatic differentiation). The model reported RMSE values of  $\sim 10^{-2}$  eV/atom for energies and  $10^{-2}$ – $10^{-3}$  eV/Å for forces, and reproduced graphene's stress–strain response (Young's modulus  $\approx$  1.056 TPa and Poisson's ratio  $\approx$  0.183) while also capturing phonon dispersion and strain-induced vibrational frequency shifts, enabling large-scale simulations with near ab initio accuracy.

In multicomponent nanocomposites, dataset size and interpretability become central. Wu et al. [86] integrated ML with MD tensile simulations (700 runs) to predict Young's modulus, yield strength, and toughness for HEA/graphene systems across compositions and temperatures. After reducing 59 descriptors to 21 features using principal component analysis, five models (XGBoost, Light Gradient Boosting Machine, random forest, AdaBoost, and decision tree) were trained with 10-fold cross-validation and grid-search optimization. XGBoost and Light Gradient Boosting Machine performed best, with  $R^2 > 0.90$  for Young's modulus and  $R^2 > 0.85$  for toughness, while yield strength predictions were lower ( $R^2 \approx 0.55$ – $0.60$ ). SHapley Additive exPlanations (SHAP) analysis identified temperature and alloy composition as the most influential inputs, illustrating how explainable tools can support mechanistic interpretation alongside prediction.

Several experimental studies on graphene-enhanced cementitious materials likewise report strong predictive performance with ensemble models. Fawad et al. [87] trained decision tree, CatBoost, Light Gradient Boosting Machine, and Adaptive Neuro-Fuzzy Inference System (ANFIS) models on 172 experimental samples to predict compressive strength, using inputs such as nanoplatelet diameter, thickness, content, water-to-cement ratio, curing age, ultrasonication time, and sand content. CatBoost achieved the best performance ( $R = 0.9999$ , MAE = 0.0704 MPa, RMSE = 0.0979 MPa), and SHAP analysis showed graphene thickness as the most influential feature (peak SHAP value +9.39). In a closely related dataset, Alahmari and Arif [88] compared XGB, LGB, ANN, and KNN on 172 samples and reported that XGB achieved  $R^2 = 0.98$  (training) and 0.94 (testing), with average prediction errors of about 1.97 MPa (training) and 3.21 MPa (testing) and uncertainty levels below 8%, again highlighting the strong performance of Gradient Boosting approaches for compressive strength prediction.

Vences-Reynoso et al. [89] investigated the use of ML models to reduce the high computational cost of geometric optimization of CNTs in atomistic simulations. The main objective was to generate pre-optimized CNT atomic geometries that accelerate subsequent first-principles optimization using the CASTEP code. The authors employed three supervised deep learning models: a multilayer perceptron (MLP), a one-dimensional CNN, and a bi-directional long short-term memory network (LSTM). The input to the models consisted of the initial atomic coordinates ( $x, y, z$ ) of CNTs with different chiralities and sizes, while the output was the optimized atomic coordinates obtained from CASTEP calculations. All models were trained using the Adamax optimizer with early stopping. The ML-predicted structures were then used as initial guesses for final CASTEP optimization. The study reported a significant reduction in computational time, ranging from about 40% to 90.62%, with the highest speed-up achieved for a 28-atom CNT using the 1D-CNN model. The results showed that MLP models were more effective for larger CNTs, while CNN-based models performed better for smaller systems, confirming that ML-assisted preoptimization is an efficient strategy for accelerating CNT geometry optimization without loss of accuracy.

In metallic nanocomposites, model choice may depend on whether elastic or strength-dominated properties are targeted. Liu et al. [63] used 336 MD-generated datasets for graphene-reinforced aluminum nanocomposites and trained ANN, SVM regression, and AdaBoost models using graphene volume fraction, orientation angle, chirality, and temperature as inputs. Gaussian SVM (G-SVM) yielded the highest accuracy for ultimate tensile strength (MSE = 0.118,  $R^2 = 0.945$ ), while ANN-30–30 provided the most accurate Young's modulus predictions ( $R^2 = 0.951$ ), reinforcing that model performance is response-dependent. These results, illustrated in Figure 1a,b, demonstrated that the optimal ML model depends strongly on the nature of the mechanical response, with different algorithms excelling in elastic versus strength-dominated properties.

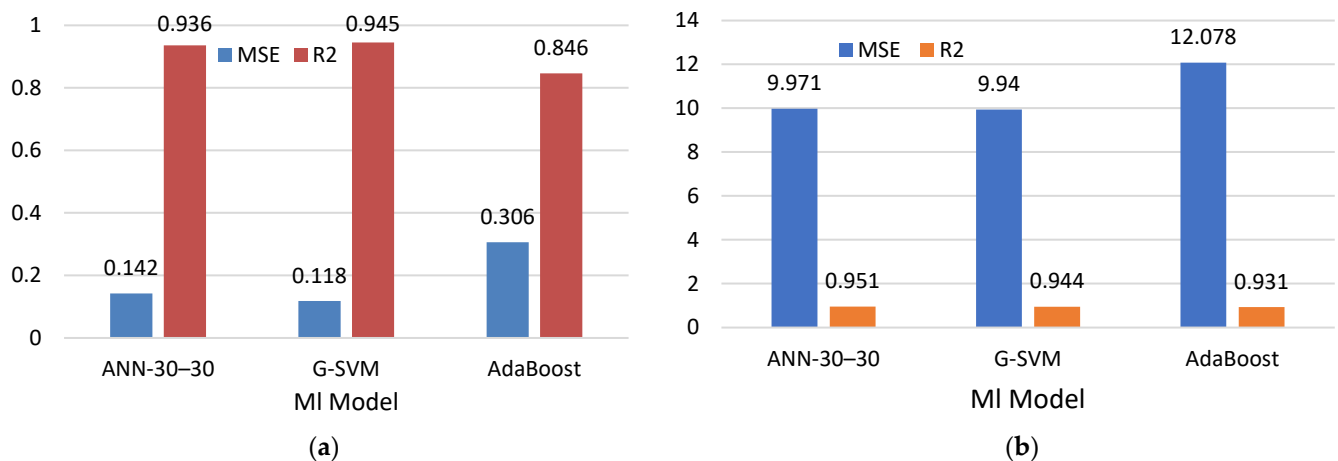


**Figure 1.** Comparison of ANN-30-30, G-SVM, and AdaBoost performance for (a) ultimate tensile strength prediction, (b) Young's modulus prediction based on data from Ref. [63].

In Ref. [84], model performance was evaluated using RMSE, MAE, and  $R^2$ . For elastic modulus estimation, the MLP exhibited strong predictive performance, achieving an  $R^2$  value of 0.85 on the test dataset with an RMSE of 2.92 GPa. The HGB and SVR models showed lower accuracy on the test data, with  $R^2$  values of 0.82 and 0.86, respectively. The reference ANN used for formula extraction achieved the highest overall accuracy, reaching an  $R^2$  of 0.87 on the test dataset and an RMSE of 2.89 GPa. In contrast, the ANN-derived analytical formula demonstrated reduced prediction accuracy, with a test  $R^2$  of 0.74, indicating a loss of precision due to model simplification. For flexural strength prediction, the results indicated a different trend. The HGB model achieved a test  $R^2$  of 0.79 with an RMSE of 1.31 MPa, while the SVR model yielded a comparable RMSE of 1.31 MPa and a test  $R^2$  of 0.78. The ANN model showed slightly lower generalization performance, with a test  $R^2$  of 0.79 and an RMSE of 1.26 MPa. The ANN-based formula for flexural strength exhibited noticeably weaker performance, with a test  $R^2$  of 0.66, confirming that the transformation of the trained neural network into an explicit mathematical expression reduced numerical accuracy. Overall, the study concluded that ANN-based models were more effective for predicting elastic modulus, whereas HGB and SVR provided more robust predictions for flexural strength.

ML has also been employed in specialized nanocomposite applications, including corrosion, electromechanical coupling, thermal transport, additive manufacturing, tribology, and porous aerogels. Zarezadeh et al. [90] predicted corrosion current density for Ni/g-C<sub>3</sub>N<sub>4</sub> coatings using ANN and ANFIS, where ANFIS achieved higher accuracy ( $R^2 = 0.99$ ) than a Levenberg–Marquardt-trained ANN ( $R^2 = 0.91$ ). Baek et al. [61] compared ANN and graph convolution networks (GCNs) for electromechanical property prediction of polypropylene/SiC nanocomposites and reported that both models reduced error substantially relative to conventional approaches, while the GCNs achieved comparable performance using fewer features and provided rapid evaluation of large RVEs. Liu et al. [91] applied XGBoost to multiscale thermal conductivity prediction using simulation-derived data and achieved  $R^2 = 0.847$  (RMSE = 0.286 W/mK; MAE = 0.116 W/mK; MAPE = 0.116%). Hossain et al. [92] used polynomial regression to predict optimal extrusion temperature as a function of speed for composite filaments, reporting predicted extrusion temperatures of 186–199 °C and experimentally improved performance, including a maximum tensile strength of 40.39 N/mm<sup>2</sup> for TiO<sub>2</sub>-reinforced filaments and insulation resistance up to 77.7 GΩ. In tribology, Öge [93] used LSBoost to predict the wear rate of PC/PBT nanocomposites with graphene nanoplatelets (GNPs) and achieved  $R^2 = 0.9922$  when contact pressure was included as an input; experimentally, 5 wt% GNP reduced wear rate

by ~86% and ~90% under 5 N and 10 N loads, respectively. Tafreshi et al. [94] trained ANN models to predict properties of polyimide aerogels, reporting strong agreement between predictions and experiments across compressive modulus, density, and porosity. For CNTs, Čanađija [95] trained a deep feedforward neural network on MD tensile tests of 818 Single-Walled Carbon Nanotube configurations, predicting Young's modulus, Poisson's ratio, UTS, and fracture strain with  $R^2 \approx 0.99$  for UTS and fracture strain and  $>0.90$  for Young's modulus and Poisson's ratio, with prediction errors generally within  $\pm 4\%$ . Finally, Golla et al. [96] compared several regressors for wear rate prediction in hybrid aluminum matrix nanocomposites and found random forest to perform best ( $R^2 = 0.9385$ ; RMSE = 0.31397; MAE = 0.23822; MSE = 0.09857).

Overall, these studies show that ML has become a practical tool for predicting mechanical properties of nanomaterials across diverse systems and response types. While ANN and SVM remain widely used, ensemble learning, graph-based models, and explainable ML tools increasingly improve robustness and interpretability. At the same time, the reported results consistently indicate that model performance depends on the specific mechanical response and data characteristics, making careful validation and problem-specific model selection essential.

## 4. ML Applications in the Mechanical Analysis of Nanostructures

### 4.1. Bending Analysis

Bending analysis plays a critical role in evaluating the mechanical performance of nanostructures [97–100]. Recent studies increasingly rely on ML-based methods to replace high-cost numerical solvers while preserving nonlinear accuracy. For example, Esfahani et al. [101] investigated the nonlinear bending behavior of nanobeams based on nonlocal strain gradient theory. The paper developed a mesh-free solution method capable of accurately solving high-order nonlinear governing equations without relying on conventional numerical solvers. Also, in Ref. [101], a PINN was used to predict the transverse deflection of a nanobeam. The spatial coordinate along the beam length served as the input, while the dimensionless deflection was taken as the output. The nonlinear governing equation and boundary condition were incorporated directly into the loss function, with spatial derivatives evaluated through automatic differentiation. The network was trained using the Adam optimizer, and Bayesian optimization was applied to tune key hyperparameters. The optimized PINN achieved very low loss values of  $4.38 \times 10^{-9}$  for simply supported beams and  $1.48 \times 10^{-7}$  for clamped beams, showing close agreement with BVP4C reference solutions. These results demonstrated that the PINN provided an accurate and robust tool for nonlinear bending analysis of nanobeams without requiring mesh generation or labeled data.

In another paper, Ma et al. [102] studied the dynamic bending response of graphene-nanoplatelet-reinforced composite (GPLRC) cylindrical microcapsules under moving micro/nanoparticles. A feedforward DNN was trained using data generated from a physics-based formulation combining modified couple stress theory and higher-order shear deformation theory. Inputs included geometric parameters, Graphene Platelet (GPL) reinforcement descriptors, boundary condition indicators, and loading parameters, while outputs were displacement and stress responses. The trained DNN achieved  $R^2 = 0.98381$  with a training RMSE of 0.69. Quantitatively, changing the GPL distribution from GPL-X to GPL-O increased axial displacement by ~24%, increasing GPL weight fraction from 0.1% to 0.3% reduced displacement by 52%, and increasing the length-scale parameter from  $R/5$  to  $R/2$  reduced displacement by up to 57%, confirming that ML can obtain coupled geometric–material effects at a fraction of the traditional computational cost. Also, Mahesh [103] investigated nonlinear deflection of smart sandwich plates with an agglomerated CNT-reinforced core and three-phase magneto-electro-elastic (TPMEE) face sheets. An

ANN trained on finite element data (higher-order shear deformation with von Kármán nonlinearity) was used to predict nonlinear central deflection from nine input parameters describing CNT distribution, interphase properties, agglomeration, and applied load. The optimal network (30 hidden neurons) achieved MSE = 1.17 and R = 0.998, with a maximum deviation of 2.36% relative to finite element results, while being  $\sim 8.85\times$  faster and requiring 67% less memory, highlighting its efficiency for nonlinear bending analysis.

Also, Zhou et al. [104] studied the transient bending response of graphene-nanoplatelet-reinforced sandwich plates under shock loading, aiming to reduce the high computational cost of repeated numerical simulations. A higher-order shear deformation formulation was first used to generate numerical data, which were then employed to train a supervised ANN as an alternative model. The ANN predicted key structural parameters, including graphene nanoplatelet weight fraction and layer thickness, to the dimensionless transient bending amplitude. The network was trained using 1895 samples over 400 epochs and achieved high accuracy, with a reported coefficient of determination  $R^2 = 0.98963$  and a training RMSE of 0.23. The results showed very close agreement between ANN predictions and numerical results; for instance, a numerical bending amplitude of 0.4168 was predicted as 0.4173, and a value of 0.0824 was predicted as 0.08236 for different graphene contents. The study concludes that the ANN-based model can reliably reproduce transient bending behavior and provides an efficient model for parametric analysis of graphene-reinforced sandwich structures.

In Ref. [54], PINNs were used as a mesh-free solver for the nonlinear governing equations of graphene-nanoplatelet-reinforced composite curved panels, covering bending (and also vibration and delamination). The PINNs took spatial coordinates and time as inputs and predicted the displacement fields needed to evaluate responses such as bending deflection, natural frequencies, and energy release rates. The nonlinear equilibrium equations (third-order shear deformation theory with von Kármán nonlinearity) were embedded in the loss function, enabling accurate solutions without mesh discretization or labeled training data.

Fang et al. [105] investigated the transient bending and dynamic response of graphene-nanoplatelet-reinforced composite (GPLRC) microplates subjected to shock loading. The aim of the study was to reduce the computational cost of higher-order finite element simulations by using an accurate ML model. In their study, the authors combined mathematical modeling with ML in four main stages. First, a higher-order finite element model was employed to simulate the transient bending response of GPLRC microplates and generate reliable numerical data. In the second stage, a higher-order mechanical formulation was established to capture nonlocal size effects and shear deformation. The third stage involved the development of a physics-informed ML method trained on the finite-element-generated data. Finally, the predicted responses were validated against numerical results to assess accuracy and generalization capability.

Moreover, in Ref. [105] a physics-informed feedforward DNN was developed and trained using data obtained from the higher-order finite element simulations. The input variables included geometric parameters, material properties, and loading characteristics of the GPLRC microplate, while the output represented bending-related quantities such as the dimensionless transverse deflection. Figure 2 presents a schematic of a general ML framework integrated with higher-order numerical modeling.

In Ref. [105], a neural network was implemented using TensorFlow and Keras and trained with the Adam optimizer using a learning rate of 0.001 and a mean squared error loss function. The dataset consisted of 198 samples generated from numerical simulations, of which 70% were used for training and 30% for testing. Due to the limited dataset size, the network was trained for up to 600 epochs to ensure convergence. Three different

network architectures were examined, and the optimal configuration included three hidden layers with 512, 128, and 10 neurons, corresponding to approximately 700 neurons in total. Model evaluation followed the train–test partitioning strategy reported in Ref. [105]. From a quantitative perspective, the optimal deep learning model achieved a minimum mean squared error of  $1.15 \times 10^{-6}$  for the training dataset and  $5.96 \times 10^{-7}$  for the testing dataset after 600 epochs. (The minor difference between the training and testing MSE values is within normal statistical variation and does not indicate overfitting or data leakage.) These results demonstrated excellent agreement between the ML predictions and the higher-order finite element solutions across different length-scale parameters and shock loading conditions. The study showed that increasing the number of hidden layers significantly reduced prediction error and improved generalization performance. Overall, the key outcome of Ref. [105] is that the proposed deep learning method can accurately reproduce the transient bending response of GPLRC microplates with very low numerical error while drastically reducing computational cost. This confirms the effectiveness of the ML model as a reliable, mesh-free model for higher-order finite element analysis in parametric and design-oriented studies of nanocomposite ultra-small plates.

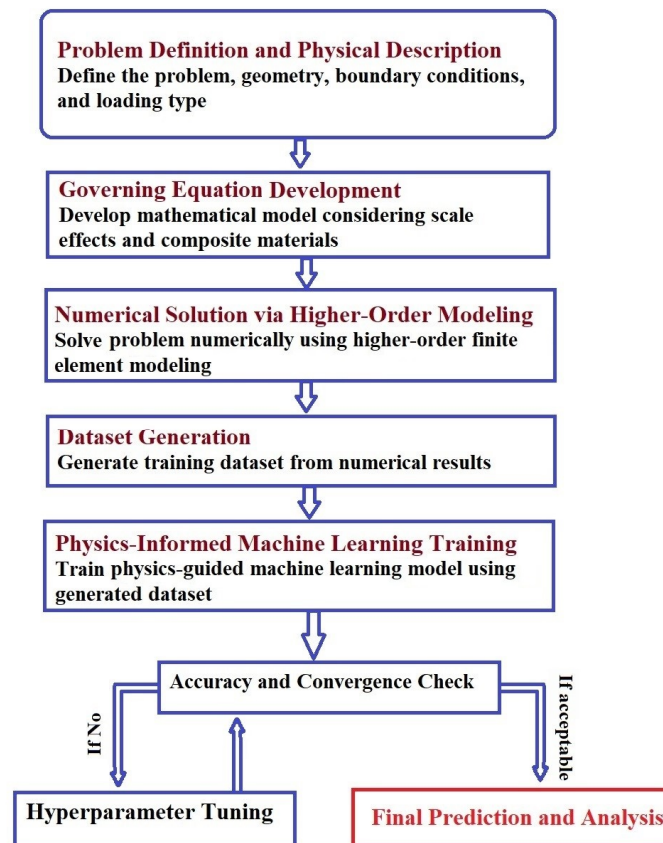


**Figure 2.** Conceptual workflow of a general ML framework commonly adopted in conjunction with higher-order numerical modeling.

#### 4.2. Buckling Analysis

ML is often used for stability and buckling analyses to reduce the cost of repeated eigenvalue calculations and parametric studies [106–109]. Recent studies consistently show that ML can accurately capture nonlinear buckling behavior which enables efficient design exploration. For example, Liu et al. [110] combined nonlocal strain gradient beam theory with an ANN to optimize the fundamental natural frequency and critical buckling load of functionally graded porous nanobeams on a Pasternak foundation. Using eight geometric and physical parameters as inputs, the ANN achieved very high accuracy ( $R^2 \approx 0.999$ ) for

both frequency and buckling load prediction. The trained model was combined with the non-dominated Sorting Genetic Algorithm (GA), leading to optimal values of  $\Omega \approx 1.17$  and  $N_{cr} \approx 1.3 \times 10^{-3}$ . In Ref. [110], the GA was employed for multi-objective optimization by maximizing the dimensionless fundamental frequency ( $\Omega$ ) and the critical buckling load ( $N_{cr}$ ) through variations in the porosity coefficient, GPL content, material gradation parameters, geometric ratios, and Pasternak foundation parameters within the ranges investigated in the numerical examples of Ref. [110]. Accordingly, the term “optimal” refers to the best solution obtained within this defined parametric design space rather than an unconstrained global optimum.

Recent ML-based studies have also investigated the buckling behavior of functionally graded nanostructures resting on other type of elastic foundations, such as the Winkler model. For example, Tariq et al. [111] employed supervised ML techniques to predict the buckling loads of bi-directional functionally graded nanobeams on a Winkler elastic foundation. In their study, a comprehensive dataset was generated using nonlocal strain gradient theory and semi-analytical solutions, and several ML models (including ANNs, support vector regression, random forest, and Gradient Boosting algorithms) were evaluated. The input features consisted of material grading indices, nonlocal and material length-scale parameters, and the non-dimensional Winkler foundation stiffness, while the outputs corresponded to the buckling loads of the nanobeam. Among the tested models, the XGBoost algorithm exhibited the best predictive performance, achieving an  $R^2$  value close to 0.99 along with very low MAE and RMSE values. These results demonstrated that ML models can accurately reproduce buckling responses governed by elastic foundation effects while significantly reducing the computational cost associated with repeated high-fidelity numerical or analytical analyses. Complementary physics-based investigations further highlight the critical role of elastic foundation modeling (particularly Winkler–Pasternak foundations) in governing the mechanical response of functionally graded nanostructures under complex loading conditions [22].

At the material modeling level, Zhao et al. [112] examined the buckling behavior of functionally graded hydrogen-functionalized graphene-reinforced copper nanocomposite beams. The purpose was to accurately obtain the effects of graphene functionalization, reinforcement content, and temperature while reducing dependency on costly MD simulations. The authors employed genetic-programming-based symbolic regression to develop explicit micromechanics models. MD simulations were first used to generate training data for temperature-dependent material properties. The input variables of the ML model were hydrogen functionalization percentage, graphene volume fraction, and temperature, while the outputs were Young’s modulus, Poisson’s ratio, coefficient of thermal expansion, and density. The genetic programming model showed strong agreement with the MD data, achieving  $R^2$  values of about 0.95 for Young’s modulus, 0.98 for thermal expansion, 0.92 for Poisson’s ratio, and 0.99 for density, with relative errors generally below a few percent. These ML-derived property models were then incorporated into the buckling analysis of functionally graded beams using Timoshenko beam theory and the Ritz method. The results indicated that hydrogen functionalization enhanced buckling resistance; for example, beams with 5% functionalization exhibited about a 7.2% higher critical buckling load than those reinforced with pristine graphene. Increasing graphene content led to significant improvements, with up to a 107% increase in buckling load at 1.5 wt% graphene compared to pure copper beams, while higher temperatures reduced buckling resistance. Overall, the study showed that genetic-programming-based ML provided an efficient and accurate way to use nanoscale material behavior into structural buckling analysis.

Deep learning has also been applied to thermally driven buckling problems. Lu et al. [113] investigated the thermal buckling behavior of a functionally graded graphene sandwich

plate (FG-GOEAM). The purpose of their study was to improve prediction efficiency while maintaining high accuracy. The authors reported that a DNN was employed as an alternative model to replace complex finite element simulations. The ML method was based on a feedforward DNN trained using simulation data generated from the Carrera Unified Formulation. The inputs to the model included geometric parameters (such as aspect ratio and thickness ratios), material parameters (graphene weight fraction, hydrogen coverage, and material gradation), and foundation stiffness properties, while the output was the critical thermal buckling temperature difference. The results showed an excellent agreement between DNN predictions and Carrera Unified Formulation (CUF) results, with a reported coefficient of determination  $R^2 = 0.9961$  and RMSE = 0.6213 based on 4580 samples, which indicates very high predictive accuracy. The study concluded that the DNN significantly reduced computational cost while reliably capturing nonlinear thermomechanical behavior, which demonstrates its effectiveness as a data-driven tool for thermal buckling analysis of graphene-reinforced nanocomposite sandwich structures.

In a related approach, Ebrahimi and Ezzati [114] investigated the thermal buckling behavior of graphene-reinforced epoxy nanocomposite beams to improve the efficiency and accuracy of buckling predictions under temperature variations. The authors introduced an ML-based regression model to estimate the temperature-dependent Young's modulus of neat epoxy and graphene-based nanocomposites. Temperature was used as the input, and Young's modulus was selected as the output. The regression model was trained using experimental data and optimized through an iterative fitting process to obtain the best predictive performance. The reported accuracy was very high, with  $R^2$  values between 0.9987 and 0.9997 and mean relative errors below 0.0007. The ML predicted elastic moduli were then incorporated into an analytical buckling formulation based on shear deformation theory and Navier's solution. The results showed that beams reinforced with functionalized graphene exhibited higher critical buckling loads than those with epoxy or graphene oxide at low temperatures, while increasing temperature led to a noticeable reduction in buckling resistance. Overall, the study demonstrated that ML provided an efficient way to link temperature-dependent material behavior to structural buckling analysis without repeated experimental fitting.

ML-assisted buckling analysis has further been extended to smart and multifunctional nanostructures. Li et al. [115] investigated the thermal buckling behavior of functionally graded GPL-reinforced composite ultra-small plates to achieve accurate buckling predictions while significantly reducing computational cost. The authors employed modified couple stress theory together with first-order shear deformation theory, and used the Ritz method to generate high-fidelity numerical data. They reported using an ANN trained with the Levenberg–Marquardt algorithm to predict the critical thermal buckling load. The ANN inputs were the piezoelectric layer thickness, GPL length and width, and graphene weight fraction, while the output was the thermal buckling load. The network was trained on 100 datasets generated by the Ritz solution, and the optimal architecture used 11 neurons in the hidden layer, with convergence achieved at about 68 epochs. Their results showed that the ANN predictions closely matched the Ritz solutions, with maximum discrepancy of only 0.26%, and the mean square error dropped below 0.001724. The authors mentioned that the ANN method reduced computational time by more than 85% compared with the conventional Ritz-based analysis, demonstrating that the proposed ML-assisted approach provided an efficient and reliable model for thermal buckling analysis of GPL-reinforced microplates with piezoelectric layers. Similarly, Kumar et al. [116] compared three models (DNN, XGBoost, and random forest) to predict the non-dimensional critical buckling load of CNT-reinforced hybrid functionally graded plates using finite element method/Monte Carlo-generated datasets. Among them, the DNN achieved the best test performance

( $R^2 = 0.943$ ), outperforming RF ( $R^2 = 0.894$ ) and XGBoost ( $R^2 = 0.842$ ). Their parametric study further showed that CNT reinforcement markedly improved buckling resistance: at 5% CNT weight fraction, single-walled CNTs produced about 17% higher critical buckling load than multi-walled CNTs at  $n = 0.5$ , and up to 37% higher load at  $n = 10$ , confirming the strong sensitivity of stability to CNT type and grading index.

#### 4.3. Vibrational Analysis

Recent studies have increasingly focused on vibration analysis, which shows the growing importance of this research area [117,118]. Vibration analysis directly affects dynamic stability, reliability, and failure prevention; however, for complex and parameter-dependent problems, repeated analytical/numerical evaluations can be computationally expensive. This has driven increasing interest in ML-based models, which can learn nonlinear mappings between system parameters and vibration responses and deliver fast, high-accuracy predictions [119–121]. For example, Ghazwani [122] examined the vibration behavior of  $\text{Si}_3\text{N}_4$  nanobeams resting on a Pasternak viscoelastic foundation under localized thermal loading. Ghazwani [122] evaluated how partial thermal exposure, nonlocal effects, and foundation stiffness influence natural frequencies, and to develop an efficient predictive method to avoid repeated analytical calculations. They [122] employed an ANN as an alternative model trained on data generated from the analytical nonlocal elasticity solution obtained using Navier's method. The input variables for the ANN were the nonlocal parameter, heated length ratio, temperature rise, and Winkler and Pasternak foundation coefficients, while the output was the non-dimensional natural frequency. The trained ANN accurately reproduced the analytical vibration results over the full parametric range. The study reported that increasing temperature rise, heated length ratio, and nonlocal parameter led to a clear reduction in natural frequencies, whereas increasing the Winkler and Pasternak stiffness parameters resulted in higher frequencies. Although no explicit percentage errors or numerical accuracy indices were reported for the ANN predictions, the model showed very close agreement with the analytical solutions. Overall, the ML approach was applied to provide fast and reliable vibration predictions for thermally affected nanobeams while preserving the trends and accuracy of the underlying analytical formulation.

Beyond structural vibration problems, ML-based vibration analysis has also been extended to bio-nanomechanical applications. For example, Wu et al. [123] developed a deep-learning-based nanomechanical vibration analysis. Their goal was to achieve sensitive epithelial–mesenchymal transition (EMT) detection using biomechanical signals while overcoming the limitations of conventional biochemical and morphology-based methods. A hybrid CNN–LSTM model was implemented to classify EMT states from nanovibration signals measured by microcantilever sensors. The CNN component was used for automatic feature extraction from raw vibration signals, and the LSTM layer captured temporal dependencies within the data. Model training employed backpropagation, and the proposed CNN–LSTM model achieved a classification accuracy of approximately 92.5% using only 1 s of nanovibration data.

In nanostructured materials, ML is particularly valuable because size effects, nonlocal interactions, and surface phenomena strongly influence vibrational behavior [124–126]. Accordingly, recent works have explored different ML models to preserve physics-based trends while reducing runtime. For example, Mazari et al. [127] studied the thermal vibration behavior of functionally graded GPL-reinforced composite beams and aimed to predict natural frequencies with reduced computational cost. Galerkin-based solutions obtained from a higher-order beam theory were used to generate reference data for training supervised ML models. Polynomial regression, SVR, and random forest regression were

evaluated using beam slenderness ratio, GPL weight fraction, and temperature difference as inputs, while the output was the non-dimensional natural frequency. A total of 2540 samples were generated for each graphene distribution pattern, with an 80/20 train-test split. Model performance was assessed using MSE and  $R^2$ . Among the tested models, random forest showed the best generalization, achieving test  $R^2$  values above 99.9% for U and X distributions and about 99.75% for the O distribution, with MSE values on the order of  $10^{-4}$ . These results indicated that the random forest model provided an accurate and efficient model for predicting vibration frequencies under varying thermal and geometric conditions, while preserving consistency with the underlying physical formulation.

The authors of Ref. [128] analyzed the free vibration behavior of porous functionally graded plates and nanoplates using a nonlocal hyperbolic high-order shear deformation theory (HHSdT) combined with an ANN. This approach maintained high accuracy in natural-frequency prediction while reducing the computational effort of repeated analytical solutions. The governing equations were derived via Hamilton's principle and solved using Navier's method, accounting for material gradation, porosity effects, and nonlocal elasticity. The analytically obtained frequencies were then used to train a supervised ANN in MATLAB, with inputs including the power-law index, porosity parameters, thickness-to-length ratio, and nonlocal length scale, and the output being the fundamental non-dimensional frequency. The ANN predictions showed excellent agreement with the HHSdT results, which themselves deviated by no more than about 0.25–0.3% from exact three-dimensional solutions, indicating that the model preserved analytical accuracy while significantly reducing computational cost for vibration analysis and parametric studies.

Tariq et al. [129], applied boosting-based ML algorithms to predict the vibration response of porous nanobeams subjected to thermal loading. Ensemble boosting was used to improve prediction accuracy by combining multiple weak learners. Model performance was assessed using  $R^2$  and RMSE, where higher  $R^2$  values and lower RMSE indicated better agreement with reference vibration frequencies. Additional metrics, including MAE and MAPE, were reported to quantify absolute and relative prediction errors. To ensure robust generalization, K-fold cross-validation was employed by iteratively training and testing the models on different data partitions. Furthermore, SHAP analysis was used to interpret the boosting models by identifying the relative influence of material, geometric, and thermal parameters on vibration predictions. The main characteristics of the examined boosting algorithms are summarized in Table 5.

Based on the reported numerical results, XGBoost consistently exhibited the highest  $R^2$  values and the lowest RMSE values across all vibration modes, indicating superior accuracy and robustness. Light Gradient Boosting showed slightly higher error values than XGBoost but maintained very high  $R^2$  values, suggesting that it provides a good balance between accuracy and computational efficiency. In contrast, Gradient Boosting and Adaptive Boosting exhibited larger RMSE values and noticeable accuracy degradation for higher vibration modes, indicating a reduced capability to capture complex nonlinear vibration behavior. These quantitative findings demonstrate that XGBoost is the most suitable model for high-accuracy vibration frequency prediction of porous nanobeams, while Light Gradient Boosting represents an efficient alternative when computational cost is a critical consideration. The detailed numerical comparison of model performance for different vibration modes is presented in Table 6.

Chen [130] investigated the vibration and stability of submerged nanobeams with axially moving supports by combining analytical modeling, numerical analysis, and ML. The aim was to predict the fundamental natural frequency and critical stability boundary while reducing the computational cost of repeated numerical simulations. Supervised tree-based regression models were trained using data generated from a reduced-order Galerkin

formulation, with input variables covering mechanical, geometric, scale-dependent, fluid, surface, and environmental parameters. Decision tree regression and least-squares boosting tree (LSBT) models were evaluated. The decision tree achieved an RMSE of 2.1856 with a determination coefficient of 0.73 using a minimum leaf size of 6, whereas the LSBT model provided higher accuracy with an RMSE of 1.2184 and  $R = 0.92$  using 60 learners and a minimum leaf size of 30. These results showed that the LSBT model offered improved predictive accuracy and computational efficiency compared with a single decision tree and conventional numerical analysis.

**Table 5.** Summary of boosting-based ML methods used for vibration prediction based on Ref. [129].

Method	Core Idea	Learning Strategy	Key Formulation (Representative)	Main Characteristics
Gradient Boosting	Sequentially improves predictions by fitting weak learners to previous errors	Weak learners trained iteratively using gradient descent on loss function	Prediction updated by adding new learner that fits negative gradient of loss	Stable convergence, good accuracy for low vibration modes, increased error for higher modes
Light Gradient Boosting	Accelerated version of Gradient Boosting using efficient data sampling	Uses histogram-based trees, Gradient-based One-Side Sampling, and Exclusive Feature Bundling	Final model expressed as additive sum of regression trees optimized via Newton’s method	High computational efficiency, reduced memory usage, accuracy close to Gradient Boosting
Extreme Gradient Boosting (XGBoost)	Regularized boosting method to improve generalization	Adds regularization to loss function to penalize model complexity	Objective function combines loss term and regularization term	High robustness, lowest prediction errors, effective for complex nonlinear vibration behavior
Adaptive Boosting	Focuses on difficult samples by adjusting sample weights	Sample weights increased for poorly predicted instances in successive iterations	Final prediction obtained from weighted combination of weak learners	Simple implementation, sensitive to noise, reduced accuracy for higher vibration modes

**Table 6.** Performance comparison of boosting-based ML models for different vibration modes obtained based on Ref. [129].

Model	Vibration Mode	$R^2$	RMSE (rad/s)	Remark
Gradient Boosting	Mode 1	0.9985	$4.34 \times 10^8$	Good accuracy for lower-vibration mode
Gradient Boosting	Mode 4	0.9953	$4.31 \times 10^9$	Reduced accuracy for higher-vibration mode
Light Gradient Boosting	Mode 1	0.9996	$2.26 \times 10^8$	High prediction accuracy
Light Gradient Boosting	Mode 4	0.9979	$2.87 \times 10^9$	Consistent performance across modes
XGBoost	Mode 1	0.9996	$2.18 \times 10^8$	Lowest reported prediction error
XGBoost	Mode 4	0.9980	$2.79 \times 10^9$	High robustness for higher-vibration modes
Adaptive Boosting	Mode 1	0.9980	$5.07 \times 10^8$	Moderate prediction accuracy
Adaptive Boosting	Mode 4	0.9904	$5.96 \times 10^9$	Significant accuracy degradation

ML has also been used with optimization methods. For example, Tran et al. [131] investigated vibration and buckling optimization of functionally graded porous microplates by integrating numerical analysis with ML. The purpose was to increase the fundamental natural frequency and critical buckling load while accounting for material uncertainty and size effects. An ANN was trained using data generated from Ritz-based solutions and coupled with the balancing composite motion optimization (BCMO) algorithm to form a

BCMO–ANN method. The model used material properties, porosity, length-scale parameter, power-law index, geometric ratios, and boundary conditions as inputs, with normalized natural frequency and buckling load as outputs. For simply supported microplates with  $a/h = 10$  and  $\beta = 0.1$ , the BCMO–ANN predicted a mean normalized frequency of 4.4090, closely matching the Ritz–BCMO value of 4.4049, while reducing computation time from about 615 s to 10 s. These results showed that the ANN-based model significantly improved computational efficiency without compromising accuracy.

To reduce dependency on closed-form eigenvalue solutions, Das et al. [132] addressed free vibration eigenvalue problems of local and nonlocal nanobeams using PINNs. The goal was to compute natural frequencies and mode shapes governed by higher-order nonlocal beam equations without relying on analytical eigenvalue solutions. A feedforward PINN was constructed by incorporating the governing differential equation, boundary conditions, and a normalization constraint directly into the loss function, with the eigenvalue treated as a trainable parameter and optimized using the Adam algorithm. The spatial coordinate was used as the input, and the transverse displacement and eigenvalue were taken as outputs, with automatic differentiation applied to evaluate spatial derivatives. For the nonlocal cantilever beam, the PINN predicted an eigenvalue of 15.1182 compared with the analytical value of 15.1953, and for the simply supported beam, it predicted 104.496 versus 105.133, corresponding to relative errors below 1%. These results confirmed that the PINN provided an accurate and efficient approach for solving nonlocal beam eigenvalue problems without closed-form solutions.

Shakir et al. [133] presented an ML-based probabilistic method for the free vibration analysis of functionally graded porous plates reinforced with graphene nanoplatelets, with the main objective of efficiently quantifying uncertainty in natural frequencies caused by material variability while significantly reducing computational cost. The authors formulated the mechanical problem using higher-order shear deformation theory and solved it numerically via the finite element method to generate a database of natural frequencies, which was then used to train a regression-based ANN. The inputs of their ML analysis were the elastic modulus of the metal matrix, elastic modulus of graphene nanoplatelets, porosity index, and graphene weight fraction, all sampled using a normal distribution with a 10% coefficient of variation, while the output was the natural frequency of the plate. The ANN architecture was optimized by varying the number of hidden neurons, and the best performance was achieved with 15 neurons in a single hidden layer, yielding an  $R^2$  value of 1 and a minimum RMSE of 0.0002%. The trained ANN was subsequently coupled with Monte Carlo simulation to perform probabilistic vibration analysis, enabling accurate estimation of probability density and cumulative distribution functions of natural frequencies. Numerical results showed that increasing graphene weight fraction increased natural frequency, whereas higher porosity reduced it; for example, for symmetric distribution and clamped boundaries, the first natural frequency increased from 805.81 Hz (0% GNP) to 994.01 Hz (1% GNP) at zero porosity. Most importantly, the proposed ML-based probabilistic approach reduced computational time by approximately 95% compared to conventional Monte Carlo simulation (about 10 h versus 222 h for 1024 samples). This demonstrates the efficiency and suitability of the technique for uncertainty-aware vibration analysis of graphene-reinforced nanostructural plates.

Siavash et al. [134] studied the nonlinear vibration and stability behavior of fluid-conveying nano-scroll channel shells (shown in Figure 3) to improve the prediction accuracy of natural frequencies using ML models. A nonlinear theoretical model based on first-order shear deformation theory and modified couple stress theory was first developed to generate reference data. Geometric parameters, material properties, and flow-related variables were considered as input, and the natural frequencies of the first four vibration modes were

considered as outputs in Ref. [134]. Both models showed high predictive capability, with ANFIS consistently outperforming the MLP. During training, ANFIS achieved an MSE of 0.0048 and an RMSE of 0.0694, compared to 0.0077 and 0.0882 for the MLP. In the testing phase, the ANFIS errors further decreased to an MSE of 0.0016 and an RMSE of 0.0402, while the MLP yielded an MSE of 0.0021 and an RMSE of 0.0467. The coefficient of determination exceeded 0.99 for most vibration modes in both models. These results indicated that ANFIS provided more accurate and stable predictions of the nonlinear vibration response. This proves the effectiveness of ML for modeling fluid-conveying nano-scroll channel shells.

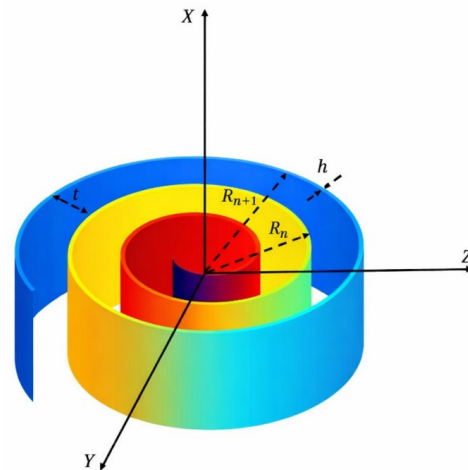


**Figure 3.** Schematic of nanochannel shell with a scroll-shaped cross-section, redrawn based on Ref. [134].

Yan et al. [135] investigated the nonlinear vibration response of GPL-reinforced nanocomposite doubly curved concrete panels subjected to thermal shock, with the main objective of accurately capturing thermally induced nonlinear frequencies while avoiding excessive computational cost from repeated numerical simulations. The authors developed a coupled thermomechanical model based on generalized differential quadrature, the Crank–Nicolson scheme, and von Kármán geometric nonlinearity, and then used ML as a verification and alternative tool. They employed an XGBoost regression model. The input variables included curvature ratios, thermal shock intensity, and material parameters such as GPL weight fraction, while the output was the dimensionless nonlinear vibration frequency. The XGBoost model was trained on data generated from the validated numerical simulations and optimized using the Sparrow Search Optimization (SSO) algorithm to tune key hyperparameters such as learning rate and subsample ratio. The optimized SSO–XGBoost model achieved high predictive accuracy, with reported  $R^2$  values generally above 0.9 and close agreement with numerical results across the studied parameter range. The results showed that increasing thermal shock reduced the nonlinear frequency, while higher curvature ratios increased it. They also showed that the ML predictions closely matched the mathematical solutions. Overall, the study demonstrated that the XGBoost-based method could reliably reproduce nonlinear vibration responses of graphene-reinforced nanocomposite panels under thermal shock with high accuracy and reduced computational effort, supporting its use as an efficient model and validation tool for complex nanostructural vibration analysis.

The authors of Ref. [136] examined the vibration behavior of graphene-oxide-based nanocomposites to provide an efficient alternative to analytical vibration analysis. The authors reported that ML was used to predict natural frequencies while reducing computational cost and modeling complexity. ANN-based models were trained using vibration data generated from analytical formulations based on higher-order shell theory. The input

variables included nanocomposite material properties (such as graphene oxide content), geometric parameters of the structure, and curvature-related factors, and the output was the natural frequency. They reported that the trained models showed very close agreement with analytical results, which shows high prediction accuracy with strong similarity between predicted and reference frequencies. These results demonstrated that ML can be effectively applied as an alternative model for vibration analysis of nanocomposite-reinforced structures, and that it makes fast and reliable predictions with accuracy.

Mazari et al. [137] investigated the free vibration behavior of GPL-reinforced composite (GPLRC) beams subjected to nonuniform magnetic fields to improve the prediction accuracy of vibration frequencies and reducing repeated analytical solutions. The authors formulated the mechanical problem using a refined higher-order beam theory and solved the equations with the Galerkin method to generate reliable reference data. A supervised multivariable linear regression model was used. The input variables were explicitly defined as the length-to-thickness ratio, GPL weight fraction, and magnetic field intensity. The output was the non-dimensional natural frequency. The trained model initially achieved an  $R^2$  value of 0.94, explaining 94% of the variance in the vibration frequencies, and after data refinement and feature–target relationship analysis, the predictive accuracy improved to  $R^2 = 0.965$  for training and  $R^2 = 0.9625$  for testing. The results showed that increasing GPL content and magnetic field intensity led to higher vibration frequencies with the GPLRC-X distribution. This caused the highest frequencies, and the GPLRC-O pattern caused the lowest. Overall, the study demonstrated that using multivariable linear regression with physics-based vibration analysis provided an efficient and accurate model for predicting the vibrational response of graphene nanocomposite beams under magnetic loading.

Belarbi et al. [138] investigated the free vibration behavior of nanoscale functionally graded material (FGM) beams to develop an accurate and computationally efficient model for predicting fundamental natural frequencies under various boundary conditions and size-dependent effects. In their paper, they used a hybrid ML method. First, they used SVR to capture the global nonlinear trend between input parameters and vibration frequency. Then an ANN was trained to learn the residual errors and refine the predictions. The input variables included geometric and material parameters such as the length-to-thickness ratio, gradient index, nonlocal parameter, Young's modulus, density, Poisson's ratio, and boundary condition indicators, and the output was the fundamental vibration frequency of the nano-FGM beam. Finite element simulations based on a parabolic shear deformation theory with nonlocal elasticity were used to generate the training and testing datasets. The study showed that hyperparameters of both an SVR and ANN were optimized using metaheuristic algorithms, including Bald Eagle Search, Puma Optimizer, Logarithmic Mean-Based Optimization, and Tribal Intelligent Evolution Optimization. Among these, the Bald Eagle Search-tuned hybrid SVR–ANN model achieved the best performance, with reported RMSE values around 0.176, NSE values close to 0.99, and variance accounted for exceeding approximately 99%, indicating very high predictive accuracy. The results demonstrated that the proposed ML method could reliably reproduce finite element vibration results and significantly reducing computational cost. This makes suitable for parametric analysis and design of nano-FGM beams.

Tariq et al. [139] examined the free vibration response of functionally graded viscoelastic nonlocal Euler–Bernoulli beams with deformable boundary conditions to develop an accurate and computationally efficient prediction method. A semi-analytical model based on nonlocal elasticity theory was first used to generate a comprehensive dataset. In their scientific article, the power-law exponent, length-to-thickness ratio, nonlocal parameter, and damping coefficient served as inputs, and the real and imaginary parts of the natural frequencies for the first three modes were treated as outputs. Several regression-based

ML models, including k-nearest neighbor, decision tree regression, XGBoost, and Light Gradient Boosting, were trained using Sobol sequence sampling. Hyperparameter tuning was performed using different optimization techniques, namely Bayesian optimization with Gaussian process (BOGP), Bayesian optimization with tree-structured Parzen estimator (BOTSPE), particle swarm optimization (PSO), and GA. The overall workflow of data generation, model training, optimization, and validation is summarized in the flowchart shown in Figure 4.

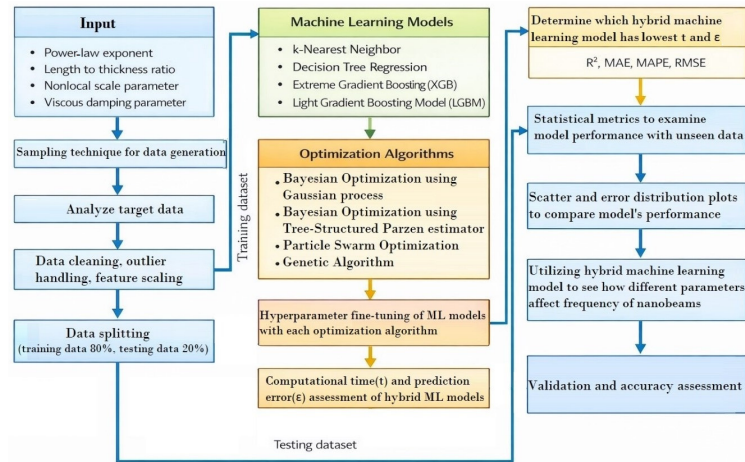


**Figure 4.** Flowchart illustrating workflow for free vibration analysis of functionally graded viscoelastic nonlocal Euler–Bernoulli beams using ML and hyperparameter optimization, redrawn based on Ref. [139].

As presented in Figures 5 and 6, the computational costs and prediction errors associated with hyperparameter optimization exhibit considerable variation across different ML models and optimization algorithms. Among the investigated techniques, BOTSPE consistently demonstrated the highest computational efficiency by achieving the shortest optimization times for all models. The minimum computational time was recorded as 11.64 s for the DTR model using BOTSPE. In contrast, PSO resulted in the highest computational cost, with the maximum optimization time of 180.4 s observed for the LGBM model. Although the GA also required relatively long optimization times, its computational cost remained lower than that of PSO in several cases. Overall, BOGP generally required more time than BOTSPE. But it was computationally more efficient than both PSO and GA for most models.

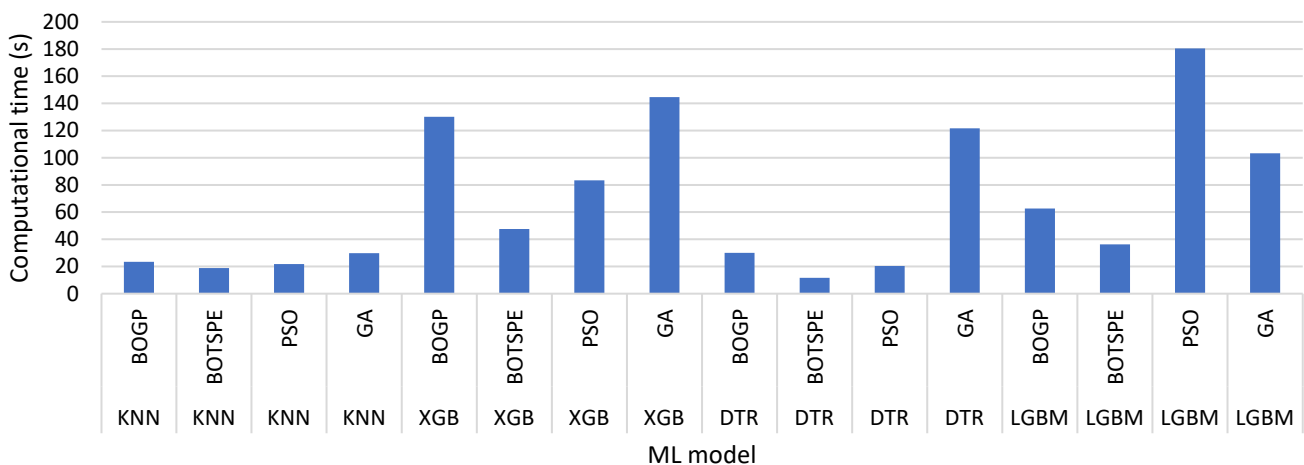


**Figure 5.** Computational costs using hyperparameter optimization among different ML models based on data from Ref. [139].

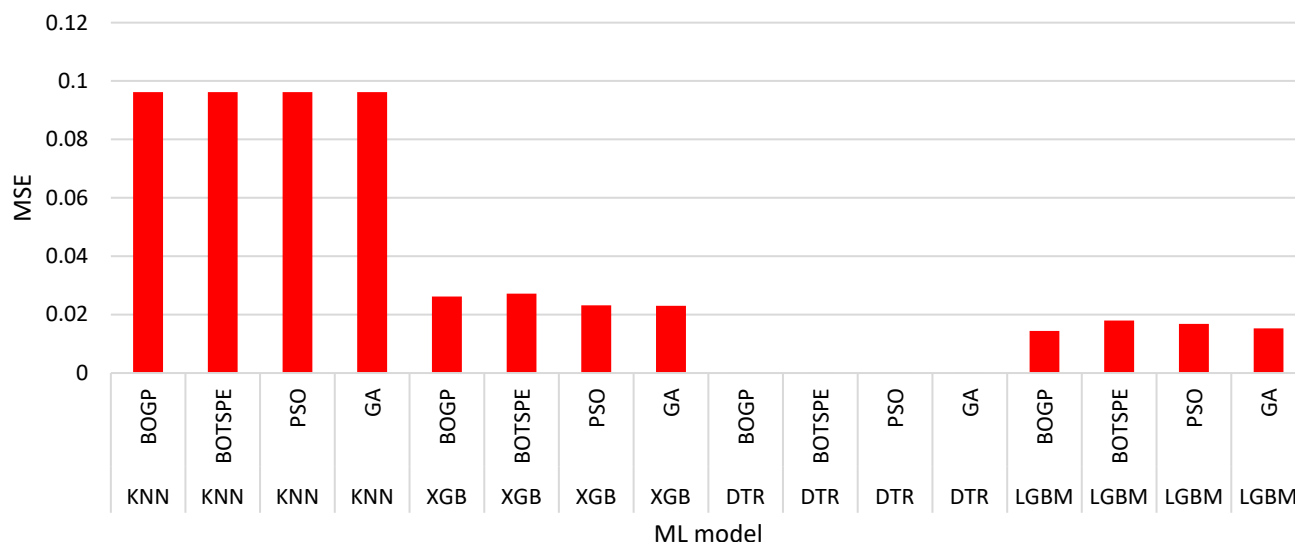


**Figure 6.** Comparison of errors using hyperparameter optimization among different ML models based on data from Ref. [139].

## 5. Discussion and Future Research Directions

The reviewed studies show that ML has become an effective tool for the mechanical analysis of nanomaterials and nanostructured systems. Across different applications (including property prediction, vibration, static analyses), ML-based models have shown strong capability in capturing complex nonlinear relationships that are difficult to resolve using classical analytical or numerical approaches alone. In particular, models trained on data generated from finite element simulations, MD calculations, or experimental measurements have significantly reduced computational cost while maintaining high predictive accuracy.

The literature shows that the predictive performance of ML models strongly depends on the nature of the mechanical problem, the quality and diversity of training data, and the choice of learning algorithm. Simple models and combined methods often provide robust predictions with relatively low computational cost, but deep learning architectures are better suited for problems involving complex microstructural features, high-dimensional parameter spaces, or strong nonlinearity. However, increased model complexity does not always guarantee superior performance, highlighting the importance of systematic model comparison, proper validation, and careful interpretation of performance metrics.

Despite the growing success of ML in nanomechanical analysis, several limitations remain. ML models are highly dependent on the quality and representativeness of training data, which are often limited or simulation-dependent at the nanoscale, reducing generalization capability. Moreover, purely data-driven approaches may lack physical interpretability, leading to unreliable predictions outside the training domain, particularly for nonlinear, stability, and failure problems. The black-box nature of many deep learning models can also hinder scientific trust. These issues highlight the importance of rigorous validation, uncertainty quantification, and the integration of physical constraints through physics-informed or hybrid ML approaches.

In addition to these limitations, several fundamental challenges remain. One of the most critical issues is the limited availability of high-quality, standardized datasets for nanoscale mechanical problems. Many existing studies rely on relatively small datasets generated from numerical simulations under specific assumptions, which can limit model generalization across different material systems, geometries, or loading conditions. Data

imbalance, noise, and inconsistency across experimental and simulation sources further complicate reliable model training and validation.

The application of ML to nanomaterials and nanostructures differs fundamentally from its use in conventional materials and macroscopic structures. At the nanoscale, mechanical behavior is strongly affected by size-dependent effects, surface and interface phenomena, nonlocal interactions, and multiscale coupling, which are often negligible at larger scales. In addition, datasets for nanomaterials are frequently limited in size and primarily generated from numerical simulations or atomistic calculations, rather than large experimental databases. As a result, ML models for nanomaterials and nanostructures require problem-specific feature selection, careful validation, and often benefit from physics-informed or hybrid learning strategies to ensure reliable and physically meaningful predictions.

Another limitation is that purely data-driven models often lack clear physical interpretability. Even when accurate predictions are obtained, the connection between the learned model and the governing nanoscale mechanical mechanisms is not always evident. This issue is particularly relevant for failure-related phenomena such as fracture, fatigue, and instability, where physically unrealistic predictions may arise outside the training domain. For this reason, recent studies focus on physics-informed and hybrid ML methods, in which governing equations, constitutive laws, or boundary conditions are embedded directly into the learning process. Such approaches have demonstrated improved robustness, extrapolation capability, and physical reliability, especially in data-scarce regimes.

Future research should focus on using ML with multiscale modeling methods to improve nanomechanical analysis. Combining atomistic simulations, continuum mechanics, and ML-based models can enable efficient information transfer across length scales and support the design of nanostructured materials with optimized mechanical performance. Second, the development of explainable and interpretable ML models is expected to play an increasingly important role, allowing researchers to identify dominant physical parameters, assess uncertainty, and establish trust in ML-assisted predictions.

Multiscale modeling represents a particularly promising area for the application of artificial intelligence and ML in solid mechanics. The inherent complexity of linking atomistic, mesoscale, and continuum descriptions, as well as the determination of effective material and structural properties, poses significant challenges for conventional modeling approaches. ML techniques offer new opportunities to learn scale-bridging relationships, approximate effective properties, and reduce the computational cost associated with multiscale simulations. Consequently, ML-based multiscale frameworks have strong potential to enhance both predictive accuracy and computational efficiency in the analysis and design of advanced materials and structural components.

Overall, ML is expected to remain a central component of next-generation nanomechanical modeling and design methods. Continued progress in data quality, physics-informed learning, interpretability, and computational efficiency will be crucial for realizing reliable, scalable, and physically consistent ML approaches for the mechanical analysis and optimization of nanomaterials and nanostructured systems.

## 6. Conclusions

This review has presented a comprehensive overview of ML applications in the mechanical analysis of nanomaterials and nanostructured systems. By examining recent studies across different nanostructures (including nanobeams, nanoplates, nanotubes, graphene-based materials, porous and functionally graded nanocomposites, and architected nanosystems), the role of ML as an effective model and complementary modeling method has been clearly demonstrated. The reviewed works show that ML approaches can

accurately predict different mechanical responses, such as property prediction, bending, vibration, and buckling, while significantly reducing computational cost compared to conventional analytical and numerical methods.

Despite these advances, practical application of ML in engineering is limited by data limitations, challenges in model transferability, and limited physical interpretability. The reviewed studies also show that high predictive accuracy alone is insufficient; careful interpretation of performance metrics, uncertainty quantification, and assessment of computational efficiency are essential for reliable use of models in nanomechanical applications.

Among the ML models examined in this study, including ANNs, SVM, and AdaBoost regression, the G-SVM provided the most accurate predictions for Young's modulus and ultimate tensile strength of graphene-reinforced aluminum nanocomposites, although it required a higher computational cost compared to the ANN and AdaBoost models.

It is also concluded that no single ML model was universally optimal and that model selection in nanoscale analysis should be property-dependent.

The main objective of using ML in the reviewed studies was to reduce computational cost, improve prediction accuracy, and simplify the analysis of complex nanoscale problems.

Overall, ML has evolved from a data-driven prediction tool into a powerful component of modern nanomechanics research, enabling efficient analysis, optimization, and design of nanostructured materials. Continued progress in data generation, physics-informed learning, model interpretability, and multiscale integration is expected to further enhance the reliability and applicability of ML approaches. With these developments, ML is likely to play an important role in next-generation mechanical modeling methods for nanomaterials, connecting atomistic simulations, continuum mechanics, and practical engineering design.

**Author Contributions:** Conceptualization, M.S. and P.G.; methodology, M.S., P.G. and G.J.; formal analysis, P.G.; investigation, M.S. and G.J.; writing—original draft preparation, M.S.; writing—review and editing, A.P. and P.G.; supervision, A.P.; project administration, P.G. All authors have read and agreed to the published version of the manuscript.

**Funding:** This research received no external funding.

**Institutional Review Board Statement:** Not applicable.

**Informed Consent Statement:** Not applicable.

**Data Availability Statement:** The original contributions presented in this study are included in the article. Further inquiries can be directed to the corresponding authors.

**Conflicts of Interest:** The authors declare no conflicts of interest.

## References

1. Vignesh, J.; Ramesh, B.; Xavier, J.R. A comprehensive review of materials, processing, and performance of nano-doped engineered geopolymer composites for construction applications. *Case Stud. Constr. Mater.* **2025**, *23*, e05625. [[CrossRef](#)]
2. Bin Hashim, R.M.; Almkhadmeh, M.N.; Onaizi, S.A. Recent developments in NO<sub>x</sub> capture and conversion using nano-structured materials: A comprehensive review. *J. Environ. Chem. Eng.* **2025**, *13*, 117602. [[CrossRef](#)]
3. Huang, H.; Wang, C.; Liu, G. Tailoring the interface structures of micro-nano materials for electrochemical and biomedical applications: A review. *J. Alloys Compd.* **2025**, *1035*, 181532. [[CrossRef](#)]
4. Elmasry, A.; Azoti, W.; El-Safty, S.A.; Elmarakbi, A. A comparative review of multiscale models for effective properties of nano- and micro-composites. *Prog. Mater. Sci.* **2023**, *132*, 101022. [[CrossRef](#)]
5. Brown, K.A.; Brittman, S.; Maccaferri, N.; Jariwala, D.; Celano, U. Machine Learning in Nanoscience: Big Data at Small Scales. *Nano Lett.* **2020**, *20*, 2–10. [[CrossRef](#)]
6. Mim, J.J.; Mamun, A.A.; Nayem, M.H.; Mahmud, S.; Nath, A.; Rahman, S.M.M.; Fidal, S.A.; Hossain, N. Machine Learning-Driven Advances in Nanotechnology: From Materials Design to Process Optimization—A Review. *Mater. Today Commun.* **2025**, *50*, 114485. [[CrossRef](#)]

7. Logakannan, K.P.; Guven, I.; Odegard, G.; Wang, K.; Zhang, C.; Liang, Z.; Spear, A. A review of artificial intelligence (AI)-based applications to nanocomposites. *Compos. Part A Appl. Sci. Manuf.* **2025**, *197*, 109027. [[CrossRef](#)]
8. Gomez-Flores, A.; Cho, H.; Hong, G.; Nam, H.; Kim, H.; Chung, Y. A critical review on machine learning applications in fiber composites and nanocomposites: Towards a control loop in the chain of processes in industries. *Mater. Des.* **2024**, *245*, 113247. [[CrossRef](#)]
9. Henkes, A.; Wessels, H.; Mahnken, R. Physics informed neural networks for continuum micromechanics. *Comput. Methods Appl. Mech. Eng.* **2022**, *393*, 114790. [[CrossRef](#)]
10. Dong, C. Effective Elastic Modulus of Wavy Single-Wall Carbon Nanotubes. *C* **2023**, *9*, 54. [[CrossRef](#)]
11. Madikere Raghunatha Reddy, A.K.; Darwiche, A.; Reddy, M.V.; Zaghbi, K. Review on Advancements in Carbon Nanotubes: Synthesis, Purification, and Multifaceted Applications. *Batteries* **2025**, *11*, 71. [[CrossRef](#)]
12. Al Faruque, M.A.; Syduzzaman, M.; Sarkar, J.; Bilisik, K.; Naebe, M. A Review on the Production Methods and Applications of Graphene-Based Materials. *Nanomaterials* **2021**, *11*, 2414. [[CrossRef](#)]
13. Singh, H.; Budiarto, H.A.; Singh, B.; Kumar, K.; Gupta, R.; Bhowmik, A.; Santhosh, A.J. Graphene for next-generation technologies: Advances in properties, applications, and industrial integration. *Results Eng.* **2025**, *27*, 106865. [[CrossRef](#)]
14. Rahman, M.M.; Khan, K.H.; Parvez, M.M.; Irizarry, N.; Uddin, M.N. Polymer Nanocomposites with Optimized Nanoparticle Dispersion and Enhanced Functionalities for Industrial Applications. *Processes* **2025**, *13*, 994. [[CrossRef](#)]
15. Yim, Y.-J.; Yoon, Y.-H.; Kim, S.-H.; Lee, J.-H.; Chung, D.-C.; Kim, B.-J. Carbon Nanotube/Polymer Composites for Functional Applications. *Polymers* **2025**, *17*, 119. [[CrossRef](#)] [[PubMed](#)]
16. Kim, H.J.; Cho, J.-R. In-Depth Study on the Application of a Graphene Platelet-reinforced Composite to Wind Turbine Blades. *Materials* **2024**, *17*, 3907. [[CrossRef](#)]
17. Sadeghian, M.; Jamil, A.; Palevicius, A.; Janusas, G.; Naginevicius, V. The Nonlinear Bending of Sector Nanoplate via Higher-Order Shear Deformation Theory and Nonlocal Strain Gradient Theory. *Mathematics* **2024**, *12*, 1134. [[CrossRef](#)]
18. Sadeghian, M.; Palevicius, A.; Janusas, G. Nonlocal Strain Gradient Model for the Nonlinear Static Analysis of a Circular/Annular Nanoplate. *Micromachines* **2023**, *14*, 1052. [[CrossRef](#)]
19. Wang, L.; Chong, N.; Lei, D.; Ou, Z. Nonlinear vibration analysis of nonlocal fractional viscoelastic piezoelectric nanobeams incorporating surface effects. *Eur. J. Mech.-A/Solids* **2026**, *115*, 105840. [[CrossRef](#)]
20. Sadeghian, M.; Palevicius, A.; Griskevicius, P.; Janusas, G. Nonlinear Analysis of the Multi-Layered Nanoplates. *Mathematics* **2024**, *12*, 3545. [[CrossRef](#)]
21. Sadeghian, M.; Palevicius, A.; Janusas, G. Nonlinear Thermal/Mechanical Buckling of Orthotropic Annular/Circular Nanoplate with the Nonlocal Strain Gradient Model. *Micromachines* **2023**, *14*, 1790. [[CrossRef](#)]
22. Jayan, M.M.S.; Wang, L. Hygrothermal-Magnetic Dynamics of Functionally Graded Porous Nanobeams on Viscoelastic Foundation. *Mech. Solids* **2024**, *59*, 1744–1773. [[CrossRef](#)]
23. Sadeghian, M.; Palevicius, A.; Janusas, G. A Review of Theories and Numerical Methods in Nanomechanics for the Analysis of Nanostructures. *Mathematics* **2025**, *13*, 3626. [[CrossRef](#)]
24. Zhang, H.; Sun, W.; Zhang, Y.; Luo, H.; Ma, H.; Xu, K. Active vibration control of functionally graded graphene nanoplatelets reinforced composite plates with piezoelectric layers under multi-order excitation. *Eng. Struct.* **2025**, *322*, 119208. [[CrossRef](#)]
25. Phung-Van, P.; Hung, P.T.; Abdel Wahab, M.; Thai, C.H. Piezoelectric and piezomagnetic effects on functionally graded triply periodic minimal surface smart sandwich nanoscale plates using Chebyshev shear deformation theory. *Eng. Anal. Bound. Elem.* **2026**, *183*, 106602. [[CrossRef](#)]
26. Elshorbagy, M.H.; Gil-deCaria, M.; Martinez-Anton, J.C.; Cuadrado, A.; Sanchez-Brea, L.M.; Alda, J. Novel durable broadband absorber with hierarchical nano/micro photonic structure. *Surf. Interfaces* **2025**, *75*, 107728. [[CrossRef](#)]
27. Cai, J.; Seyedkanani, A.; Shahryari, B.; Lin, H.-C.; Akbarzadeh, A. Piezoelectric tuning of thermal conductivity in nano-architected gallium nitride metamaterials. *Int. J. Heat Mass Transf.* **2026**, *256*, 127911. [[CrossRef](#)]
28. Crook, C.; Bauer, J.; Guell Izard, A.; Santos de Oliveira, C.; Martins de Souza e Silva, J.; Berger, J.B.; Valdevit, L. Plate-nanolattices at the theoretical limit of stiffness and strength. *Nat. Commun.* **2020**, *11*, 1579. [[CrossRef](#)]
29. Sadeghian, M.; Palevicius, A.; Sablinskas, J.; Griskevicius, P. From Pixels to Predictions: Integrating Machine Learning and Digital Image Correlation for Damage Identification in Engineering Materials. *Materials* **2026**, *19*, 77. [[CrossRef](#)]
30. Liu, S.; Ma, M.; Su, C.; Zhang, Q.; Kang, Y. Coordinated physics-integrated machine learning and its application in tunnel engineering. *Eng. Appl. Artif. Intell.* **2026**, *166*, 113698. [[CrossRef](#)]
31. Davoodi, S.; Wood, D.A.; Al-Shargabi, M.; Vanovskiy, V.; Rukavishnikov, V.; Burnaev, E. Emerging applications of physics-informed and physics-guided machine learning in geoenery science: A review. *Commun. Nonlinear Sci. Numer. Simul.* **2026**, *154*, 109551. [[CrossRef](#)]
32. Diao, S.; Wu, Q.; Li, S.; Xu, G.; Ren, X.; Tan, L.; Jiang, G.; Song, P.; Meng, X. From synthesis to properties: Expanding the horizons of machine learning in nanomaterials research. *Mater. Horiz.* **2025**, *12*, 4133–4164. [[CrossRef](#)] [[PubMed](#)]

33. Sadeghian, M.; Palevicius, A.; Janusas, G. A Comprehensive Review of Machine-Learning Approaches for Crystal Structure/Property Prediction. *Crystals* **2025**, *15*, 925. [[CrossRef](#)]
34. Tripathy, A.; Patne, A.Y.; Mohapatra, S.; Mohapatra, S.S. Convergence of Nanotechnology and Machine Learning: The State of the Art, Challenges, and Perspectives. *Int. J. Mol. Sci.* **2024**, *25*, 12368. [[CrossRef](#)]
35. Yang, L.; Wang, H.; Leng, D.; Fang, S.; Yang, Y.; Du, Y. Machine learning applications in nanomaterials: Recent advances and future perspectives. *Chem. Eng. J.* **2024**, *500*, 156687. [[CrossRef](#)]
36. Zhao, Y.; Li, H.; Zhou, H.; Attar, H.R.; Pfaff, T.; Li, N. A review of graph neural network applications in mechanics-related domains. *Artif. Intell. Rev.* **2024**, *57*, 315. [[CrossRef](#)]
37. Ercument, D.B.; Safaei, B.; Sahmani, S.; Zeeshan, Q. Machine Learning and Optimization Algorithms for Vibration, Bending and Buckling Analyses of Composite/Nanocomposite Structures: A Systematic and Comprehensive Review. *Arch. Comput. Methods Eng.* **2025**, *32*, 1679–1731. [[CrossRef](#)]
38. Hawthorne, F.; Raulino, P.R.E.; Pelá, R.R.; Woellner, C.F. Efficient and Accurate Machine Learning Interatomic Potential for Graphene: Capturing Stress–Strain and Vibrational Properties. *J. Phys. Chem. C* **2025**, *129*, 16319–16326. [[CrossRef](#)]
39. Wu, Y.; Sicard, B.; Gadsden, S.A. Physics-informed machine learning: A comprehensive review on applications in anomaly detection and condition monitoring. *Expert Syst. Appl.* **2024**, *255*, 124678. [[CrossRef](#)]
40. Ahmadi, M.; Biswas, D.; Lin, M.; Vrionis, F.D.; Hashemi, J.; Tang, Y. Physics-informed machine learning for advancing computational medical imaging: Integrating data-driven approaches with fundamental physical principles. *Artif. Intell. Rev.* **2025**, *58*, 297. [[CrossRef](#)]
41. Sharma, H.; Arora, G.; Singh, M.K.; Ayyappan, V.; Bhowmik, P.; Rangappa, S.M.; Siengchin, S. Review of machine learning approaches for predicting mechanical behavior of composite materials. *Discov. Appl. Sci.* **2025**, *7*, 1238. [[CrossRef](#)]
42. Gokcekuyu, Y.; Ekinci, F.; Guzel, M.S.; Acici, K.; Aydin, S.; Asuroglu, T. Artificial Intelligence in Biomaterials: A Comprehensive Review. *Appl. Sci.* **2024**, *14*, 6590. [[CrossRef](#)]
43. Vergara, D.; Lampropoulos, G.; Fernández-Arias, P.; Antón-Sancho, Á. Artificial Intelligence Reinventing Materials Engineering: A Bibliometric Review. *Appl. Sci.* **2024**, *14*, 8143. [[CrossRef](#)]
44. Akmanov, I.S.; Lomov, S.V.; Spasennykh, M.Y.; Abaimov, S.G. Machine learning for nano-level defect detection in aligned random carbon nanotubes-reinforced electrically conductive nanocomposite. *Compos. Struct.* **2025**, *352*, 118651. [[CrossRef](#)]
45. Wang, H.; Cao, H.; Yang, L. Machine Learning-Driven Multidomain Nanomaterial Design: From Bibliometric Analysis to Applications. *ACS Appl. Nano Mater.* **2024**, *7*, 26579–26600. [[CrossRef](#)]
46. Chota, A.; Abrahamse, H.; George, B.P. Nano-enhanced photodynamic therapy and machine learning: Advancements, challenges, and future directions. *Biomed. Pharmacother.* **2025**, *193*, 118710. [[CrossRef](#)]
47. Chicco, D.; Warrens, M.J.; Jurman, G. The coefficient of determination R-squared is more informative than SMAPE, MAE, MAPE, MSE and RMSE in regression analysis evaluation. *PeerJ Comput. Sci.* **2021**, *7*, e623. [[CrossRef](#)]
48. Zhang, L.; Wan, Y.; Shibuta, Y.; Huang, X. Progress in machine learning interatomic potential and its applications in materials science. *Prog. Nat. Sci. Mater. Int.* **2025**, *35*, 1079–1104. [[CrossRef](#)]
49. Maleki, S.; Mousavifard, M.; Karimi-Jashni, A. Modeling of the Ni(II) removal from aqueous solutions by ion exchange resin: Comparison of various machine learning approaches. *Chem. Eng. J. Adv.* **2026**, *25*, 100987. [[CrossRef](#)]
50. Baptista, M.L.; Panse, S.; Santos, B.F. Revision and implementation of metrics to evaluate the performance of prognostics models. *Measurement* **2024**, *236*, 115038. [[CrossRef](#)]
51. Hassanat, A.B.; Alqaralleh, M.K.; Tarawneh, A.S.; Almohammadi, K.; Alamri, M.; Alzahrani, A.; Altarawneh, G.A.; Alhalaseh, R. A Novel Outlier-Robust Accuracy Measure for Machine Learning Regression Using a Non-Convex Distance Metric. *Mathematics* **2024**, *12*, 3623. [[CrossRef](#)]
52. Khoshvaght, H.; Permala, R.R.; Razmjou, A.; Khiadani, M. A critical review on selecting performance evaluation metrics for supervised machine learning models in wastewater quality prediction. *J. Environ. Chem. Eng.* **2025**, *13*, 119675. [[CrossRef](#)]
53. Aboal-Somoza, M.; Crujeiras, R.M. Misuse of Linear Regression Technique in Analytical Chemistry? *J. Chem. Educ.* **2024**, *101*, 1062–1070. [[CrossRef](#)]
54. Cao, X.; Yang, X.; Fan, L.; Habibi, M.; Albaijan, I. Delamination, frequency, and bending analysis of GPLRC curved panel with initial crack via machine learning and three-dimensional layerwise theory. *Thin-Walled Struct.* **2025**, *217*, 113503. [[CrossRef](#)]
55. Baig, N.; Kammakakam, I.; Falath, W. Nanomaterials: A review of synthesis methods, properties, recent progress, and challenges. *Mater. Adv.* **2021**, *2*, 1821–1871. [[CrossRef](#)]
56. Hughes, K.J.; Ganesan, M.; Tenchov, R.; Iyer, K.A.; Ralhan, K.; Diaz, L.L.; Bird, R.E.; Ivanov, J.; Zhou, Q.A. Nanoscience in Action: Unveiling Emerging Trends in Materials and Applications. *ACS Omega* **2025**, *10*, 7530–7548. [[CrossRef](#)]
57. Harish, V.; Tewari, D.; Gaur, M.; Yadav, A.B.; Swaroop, S.; Bechelany, M.; Barhoum, A. Review on Nanoparticles and Nanostructured Materials: Bioimaging, Biosensing, Drug Delivery, Tissue Engineering, Antimicrobial, and Agro-Food Applications. *Nanomaterials* **2022**, *12*, 457. [[CrossRef](#)]

58. Vargo, E.; Dahl, J.C.; Evans, K.M.; Khan, T.; Alivisatos, P.; Xu, T. Using Machine Learning to Predict and Understand Complex Self-Assembly Behaviors of a Multicomponent Nanocomposite. *Adv. Mater.* **2022**, *34*, 2203168. [[CrossRef](#)]
59. Li, W.; Yang, T.; Liu, C.; Huang, Y.; Chen, C.; Pan, H.; Xie, G.; Tai, H.; Jiang, Y.; Wu, Y.; et al. Optimizing Piezoelectric Nanocomposites by High-Throughput Phase-Field Simulation and Machine Learning. *Adv. Sci.* **2022**, *9*, 2105550. [[CrossRef](#)]
60. Bahmani, A.; Nooraie, R.Y.; Willett, T.L.; Montesano, J. A sequential mobile packing algorithm for micromechanical assessment of heterogeneous materials. *Compos. Sci. Technol.* **2023**, *237*, 110008. [[CrossRef](#)]
61. Baek, K.; Hwang, T.; Lee, W.; Chung, H.; Cho, M. Deep learning aided evaluation for electromechanical properties of complexly structured polymer nanocomposites. *Compos. Sci. Technol.* **2022**, *228*, 109661. [[CrossRef](#)]
62. Shen, Z.-H.; Bao, Z.-W.; Cheng, X.-X.; Li, B.-W.; Liu, H.-X.; Shen, Y.; Chen, L.-Q.; Li, X.-G.; Nan, C.-W. Designing polymer nanocomposites with high energy density using machine learning. *npj Comput. Mater.* **2021**, *7*, 110. [[CrossRef](#)]
63. Liu, J.; Zhang, Y.; Zhang, Y.; Kitipornchai, S.; Yang, J. Machine learning assisted prediction of mechanical properties of graphene/aluminium nanocomposite based on molecular dynamics simulation. *Mater. Des.* **2022**, *213*, 110334. [[CrossRef](#)]
64. Bahtiri, B.; Arash, B.; Scheffler, S.; Jux, M.; Rolfes, R. A machine learning-based viscoelastic–viscoplastic model for epoxy nanocomposites with moisture content. *Comput. Methods Appl. Mech. Eng.* **2023**, *415*, 116293. [[CrossRef](#)]
65. Jia, Y.; Hou, X.; Wang, Z.; Hu, X. Machine Learning Boosts the Design and Discovery of Nanomaterials. *ACS Sustain. Chem. Eng.* **2021**, *9*, 6130–6147. [[CrossRef](#)]
66. Timoshenko, J.; Wrasman, C.J.; Luneau, M.; Shirman, T.; Cargnello, M.; Bare, S.R.; Aizenberg, J.; Friend, C.M.; Frenkel, A.I. Probing Atomic Distributions in Mono- and Bimetallic Nanoparticles by Supervised Machine Learning. *Nano Lett.* **2019**, *19*, 520–529. [[CrossRef](#)]
67. Ali, A.; Park, H.; Mall, R.; Aissa, B.; Sanvito, S.; Bensmail, H.; Belaidi, A.; El-Mellouhi, F. Machine Learning Accelerated Recovery of the Cubic Structure in Mixed-Cation Perovskite Thin Films. *Chem. Mater.* **2020**, *32*, 2998–3006. [[CrossRef](#)]
68. Takahashi, K.; Takahashi, L. Data Driven Determination in Growth of Silver from Clusters to Nanoparticles and Bulk. *J. Phys. Chem. Lett.* **2019**, *10*, 4063–4068. [[CrossRef](#)]
69. Koohi-Moghadam, M.; Wang, H.; Wang, Y.; Yang, X.; Li, H.; Wang, J.; Sun, H. Predicting disease-associated mutation of metal-binding sites in proteins using a deep learning approach. *Nat. Mach. Intell.* **2019**, *1*, 561–567. [[CrossRef](#)]
70. Yan, X.; Sedykh, A.; Wang, W.; Yan, B.; Zhu, H. Construction of a web-based nanomaterial database by big data curation and modeling friendly nanostructure annotations. *Nat. Commun.* **2020**, *11*, 2519. [[CrossRef](#)]
71. Russo, D.P.; Yan, X.; Shende, S.; Huang, H.; Yan, B.; Zhu, H. Virtual Molecular Projections and Convolutional Neural Networks for the End-to-End Modeling of Nanoparticle Activities and Properties. *Anal. Chem.* **2020**, *92*, 13971–13979. [[CrossRef](#)]
72. Liu, G.; Yan, X.; Sedykh, A.; Pan, X.; Zhao, X.; Yan, B.; Zhu, H. Analysis of model PM2.5-induced inflammation and cytotoxicity by the combination of a virtual carbon nanoparticle library and computational modeling. *Ecotoxicol. Environ. Saf.* **2020**, *191*, 110216. [[CrossRef](#)] [[PubMed](#)]
73. Maksov, A.; Dyck, O.; Wang, K.; Xiao, K.; Geohegan, D.B.; Sumpter, B.G.; Vasudevan, R.K.; Jesse, S.; Kalinin, S.V.; Ziatdinov, M. Deep learning analysis of defect and phase evolution during electron beam-induced transformations in WS<sub>2</sub>. *npj Comput. Mater.* **2019**, *5*, 12. [[CrossRef](#)]
74. Carrera, D.; Manganini, F.; Boracchi, G.; Lanzarone, E. Defect Detection in SEM Images of Nanofibrous Materials. *IEEE Trans. Ind. Inform.* **2017**, *13*, 551–561. [[CrossRef](#)]
75. Iwasaki, Y.; Takeuchi, I.; Stanev, V.; Kusne, A.G.; Ishida, M.; Kirihara, A.; Ihara, K.; Sawada, R.; Terashima, K.; Someya, H.; et al. Machine-learning guided discovery of a new thermoelectric material. *Sci. Rep.* **2019**, *9*, 2751. [[CrossRef](#)]
76. Copp, S.M.; Swasey, S.M.; Gorovits, A.; Bogdanov, P.; Gwinn, E.G. General Approach for Machine Learning-Aided Design of DNA-Stabilized Silver Clusters. *Chem. Mater.* **2020**, *32*, 430–437. [[CrossRef](#)]
77. Copp, S.M.; Gorovits, A.; Swasey, S.M.; Gudibandi, S.; Bogdanov, P.; Gwinn, E.G. Fluorescence Color by Data-Driven Design of Genomic Silver Clusters. *ACS Nano* **2018**, *12*, 8240–8247. [[CrossRef](#)]
78. Yang, H.; Zhang, Z.; Zhang, J.; Zeng, X.C. Machine learning and artificial neural network prediction of interfacial thermal resistance between graphene and hexagonal boron nitride. *Nanoscale* **2018**, *10*, 19092–19099. [[CrossRef](#)]
79. Fernandez, M.; Bilić, A.; Barnard, A.S. Machine learning and genetic algorithm prediction of energy differences between electronic calculations of graphene nanoflakes. *Nanotechnology* **2017**, *28*, 38LT03. [[CrossRef](#)]
80. Fernandez, M.; Shi, H.; Barnard, A.S. Geometrical features can predict electronic properties of graphene nanoflakes. *Carbon* **2016**, *103*, 142–150. [[CrossRef](#)]
81. Sigmund, G.; Gharasoo, M.; Hüffer, T.; Hofmann, T. Deep Learning Neural Network Approach for Predicting the Sorption of Ionizable and Polar Organic Pollutants to a Wide Range of Carbonaceous Materials. *Environ. Sci. Technol.* **2020**, *54*, 4583–4591. [[CrossRef](#)] [[PubMed](#)]
82. Findlay, M.R.; Freitas, D.N.; Mobed-Miremadi, M.; Wheeler, K.E. Machine learning provides predictive analysis into silver nanoparticle protein corona formation from physicochemical properties. *Environ. Sci. Nano* **2018**, *5*, 64–71. [[CrossRef](#)] [[PubMed](#)]

83. Guo, Y.; Zhang, W.; Li, P.; Zhao, Y.; Mu, Z.; Yang, Z. Machine Learning-Enhanced Nanoindentation for Characterizing Micromechanical Properties and Mineral Control Mechanisms of Conglomerate. *Appl. Sci.* **2025**, *15*, 9541. [CrossRef]
84. Okasha, N.M.; Mirrashid, M.; Naderpour, H.; Ciftcioglu, A.O.; Meddage, D.P.P.; Ezami, N. Machine learning approach to predict the mechanical properties of cementitious materials containing carbon nanotubes. *Dev. Built Environ.* **2024**, *19*, 100494. [CrossRef]
85. Luo, K.; Luo, W.; Zuo, J.; Xiao, J.; Jiang, T.; Huang, L.; Zhang, W. Machine learning for predicting tensile properties in graphene-reinforced polyethylene composites. *Mater. Today Commun.* **2025**, *47*, 113053. [CrossRef]
86. Wu, Q.; Gao, T.; Liu, G.; Ma, Y. Machine learning-assisted prediction of mechanical properties of high-entropy alloy/graphene nanocomposite. *Mater. Today Commun.* **2024**, *40*, 109663. [CrossRef]
87. Fawad, M.; Alabduljabbar, H.; Farooq, F.; Najeh, T.; Gamil, Y.; Ahmed, B. Indirect prediction of graphene nanoplatelets-reinforced cementitious composites compressive strength by using machine learning approaches. *Sci. Rep.* **2024**, *14*, 14252. [CrossRef]
88. Alahmari, T.S.; Arif, K. Machine learning approaches to predict the strength of graphene nanoplatelets concrete: Optimization and hyper tuning with graphical user interface. *Mater. Today Commun.* **2024**, *40*, 109946. [CrossRef]
89. Vences-Reynoso, L.J.; Villanueva-Vasquez, D.; Alejo-Eleuterio, R.; Del Razo-López, F.; Martínez-Gallegos, S.M.; Granda-Gutiérrez, E.E. Evaluation of Neural Networks for Improved Computational Cost in Carbon Nanotubes Geometric Optimization. *Modelling* **2025**, *6*, 36. [CrossRef]
90. Zarezadeh, A.; Shishesaz, M.R.; Ravanavard, M.; Ghobadi, M.; Zareipour, F.; Mahdavian, M. Electrochemical and Mechanical Properties of Ni/g-C<sub>3</sub>N<sub>4</sub> Nanocomposite Coatings with Enhanced Corrosion Protective Properties: A Case Study for Modeling the Corrosion Resistance by ANN and ANFIS Models. *J. Appl. Comput. Mech.* **2023**, *9*, 590–606.
91. Liu, B.; Liu, P.; Wang, Y.; Li, Z.; Lv, H.; Lu, W.; Olofsson, T.; Rabczuk, T. Explainable machine learning for multiscale thermal conductivity modeling in polymer nanocomposites with uncertainty quantification. *Compos. Struct.* **2025**, *370*, 119292. [CrossRef]
92. Hossain, M.I.; Chowdhury, M.A.; Mahamud, S.; Saha, R.K.; Zahid, M.S.; Ferdous, J.; Hossain, N.; Mobarak, M.H. Electro-mechanical analysis of nanostructured polymer matrix composite materials for 3D printing using machine learning. *Chem. Eng. J. Adv.* **2024**, *19*, 100626. [CrossRef]
93. Özdemir Öge, T. Enhancement and Machine Learning-Based Prediction of Tribological Properties of PC/PBT/GNPs Nanocomposites. *ACS Omega* **2025**, *10*, 23639–23662. [CrossRef] [PubMed]
94. Tafreshi, O.A.; Saadatnia, Z.; Ghaffari-Mosanenzadeh, S.; Okhovatian, S.; Park, C.B.; Naguib, H.E. Machine learning-based model for predicting the material properties of nanostructured aerogels. *SPE Polym.* **2023**, *4*, 24–37. [CrossRef]
95. Čanadija, M. Deep learning framework for carbon nanotubes: Mechanical properties and modeling strategies. *Carbon* **2021**, *184*, 891–901. [CrossRef]
96. Golla, C.B.; Rao, R.N.; Ismail, S.; Özcan, M.; Prasad, P.S. Development of hybrid aluminum nanocomposites for automotive applications: An in-depth analysis using experimental approaches and predictive machine learning techniques. *J. Mater. Res. Technol.* **2025**, *36*, 4383–4399. [CrossRef]
97. Cruz, D.J.; Barbosa, M.R.; Santos, A.D.; Miranda, S.S.; Amaral, R.L. Application of Machine Learning to Bending Processes and Material Identification. *Metals* **2021**, *11*, 1418. [CrossRef]
98. Görüş, V.; Bahşi, M.M.; Çevik, M. Machine learning for the prediction of problems in steel tube bending process. *Eng. Appl. Artif. Intell.* **2024**, *133*, 108584. [CrossRef]
99. Li, J.; Lin, J.; Guan, Y.; Naceur, H.; Bao, Y.; Lu, J.; Xie, X. Thermomechanical bending of functionally graded carbon nanotubes reinforced composite plate by meshless method. *Polym. Compos.* **2024**, *45*, 13063–13075. [CrossRef]
100. Sahib, M.M.; Kovács, G. Using Artificial Neural Networks to Predict the Bending Behavior of Composite Sandwich Structures. *Polymers* **2025**, *17*, 337. [CrossRef]
101. Mirsadeghi Esfahani, S.S.; Fallah, A.; Mohammadi Aghdam, M. Physics-Informed Neural Network for Nonlinear Bending Analysis of Nano-Beams: A Systematic Hyperparameter Optimization. *Math. Comput. Appl.* **2025**, *30*, 72. [CrossRef]
102. Ma, Z.; Xing, B.; Liu, J. Dynamic analysis of GPLs reinforced microcapsules subjected to moving micro/nanoparticles using mathematical modeling and deep-neural networks. *Measurement* **2024**, *225*, 113940. [CrossRef]
103. Mahesh, V. Machine learning assisted nonlinear deflection analysis of agglomerated carbon nanotube core smart sandwich plate with three-phase magneto-electro-elastic skin. *Proc. Inst. Mech. Eng. Part L J. Mater. Des. Appl.* **2023**, *238*, 3–21. [CrossRef]
104. Zhou, X.; Chen, Y.; Abbas, M. Transient bending analysis of the graphene nanoplatelets reinforced sandwich concrete building structure validated by machine learning algorithm. *Mech. Adv. Mater. Struct.* **2025**, *32*, 260–281. [CrossRef]
105. Fang, Y.; Irfan, R.; Almadhor, A.; Abbas, M. Bending information of nanocomposites-reinforced microplate subjected to transient loading: Introducing physics-informed machine learning algorithm for solving the transient problem. *Aerosp. Sci. Technol.* **2024**, *148*, 109074. [CrossRef]
106. Gomes, G.F.; Mesquita, M.H.; Bendine, K. Predictive modeling of buckling in composite tubes: Integrating artificial neural networks for damage detection. *Mech. Adv. Mater. Struct.* **2025**, *32*, 2659–2673. [CrossRef]
107. Lee, H.G.; Sohn, J.M. A Comparative Analysis of Buckling Pressure Prediction in Composite Cylindrical Shells Under External Loads Using Machine Learning. *J. Mar. Sci. Eng.* **2024**, *12*, 2301. [CrossRef]

108. Hong, H.; Kim, W.; Kim, W.; Jeong, J.-m.; Kim, S.; Kim, S.S. Machine Learning-Driven Design Optimization of Buckling-Induced Quasi-Zero Stiffness Metastructures for Low-Frequency Vibration Isolation. *ACS Appl. Mater. Interfaces* **2024**, *16*, 17965–17972. [[CrossRef](#)]
109. Guan, W.; Zhu, Y.-m.; Bao, J.-j.; Zhang, J. Predicting buckling of carbon fiber composite cylindrical shells based on backpropagation neural network improved by sparrow search algorithm. *J. Iron Steel Res. Int.* **2023**, *30*, 2459–2470. [[CrossRef](#)]
110. Liu, H.; Basem, A.; Jasim, D.J.; Hashemian, M.; Ali Eftekhari, S.; Al-fanhrawi, H.J.; Abdullaeva, B.; Salahshour, S. Multi-objective optimization of buckling load and natural frequency in functionally graded porous nanobeams using non-dominated sorting genetic Algorithm-II. *Eng. Appl. Artif. Intell.* **2025**, *142*, 109938. [[CrossRef](#)]
111. Tariq, A.; Uzun, B.; Deliktaş, B.; Yaylı, M.Ö. A machine learning approach for buckling analysis of a bi-directional FG microbeam. *Microsyst. Technol.* **2025**, *31*, 177–198. [[CrossRef](#)]
112. Zhao, S.; Zhang, Y.; Zhang, Y.; Zhang, W.; Yang, J.; Kitipornchai, S. Buckling of functionally graded hydrogen-functionalized graphene reinforced beams based on machine learning-assisted micromechanics models. *Eur. J. Mech.-A/Solids* **2022**, *96*, 104675. [[CrossRef](#)]
113. Lu, Q.; Yang, Q.; Atif, M.; El-Meligy, M. Application of machine learning algorithm and Carrera unified formulation in thermal buckling analysis of a functionally graded graphene origami enabled auxetic metamaterial sandwich plate with an auxetic concrete foundation. *Mech. Adv. Mater. Struct.* **2025**, *32*, 5519–5534. [[CrossRef](#)]
114. Ebrahimi, F.; Ezzati, H. A Machine-Learning-Based Model for Buckling Analysis of Thermally Affected Covalently Functionalized Graphene/Epoxy Nanocomposite Beams. *Mathematics* **2023**, *11*, 1496. [[CrossRef](#)]
115. Li, M.; Lu, L.; She, G.-L.; Wang, S. Thermal post-buckling analysis of functionally graded graphene platelets reinforced composite microtubes. *Thin-Walled Struct.* **2024**, *203*, 112246. [[CrossRef](#)]
116. Kumar, R.; Kumar, A.; Ranjan Kumar, D. Buckling response of CNT based hybrid FG plates using finite element method and machine learning method. *Compos. Struct.* **2023**, *319*, 117204. [[CrossRef](#)]
117. Murari, B.; Zhao, S.; Zhang, Y.; Yang, J. Machine learning-assisted vibration analysis of graphene-origami metamaterial beams immersed in viscous fluids. *Thin-Walled Struct.* **2024**, *197*, 111663. [[CrossRef](#)]
118. Chen, Y.; Bi, S.; Zhang, E.; Fouly, A.; Awwad, E.M. Application of functionally graded graphene nanoplatelets to improve transient vibrations of the car's roof under mechanical loading: Introducing machine learning algorithm for transient problems. *Mater. Today Commun.* **2024**, *39*, 108990. [[CrossRef](#)]
119. Romanssini, M.; de Aguirre, P.C.C.; Compassi-Severo, L.; Girardi, A.G. A Review on Vibration Monitoring Techniques for Predictive Maintenance of Rotating Machinery. *Eng* **2023**, *4*, 1797–1817. [[CrossRef](#)]
120. Chu, T.; Nguyen, T.; Yoo, H.; Wang, J. A review of vibration analysis and its applications. *Heliyon* **2024**, *10*, e26282. [[CrossRef](#)]
121. Hao, J.; Yan, Q.; Wen, G.; Wang, J.; Zhao, L. Research on Vibration Measurement and Analysis Technology of Circuit Breaker Based on VMD and LSTM. *Appl. Sci.* **2025**, *15*, 13252. [[CrossRef](#)]
122. Ghazwani, M.H. Localized thermal loading effects on nanobeam vibrations resting on Pasternak foundations: Analytical and ANN surrogate approaches. *Case Stud. Therm. Eng.* **2025**, *75*, 107286. [[CrossRef](#)]
123. Wu, W.; Peng, Y.; Xu, M.; Yan, T.; Zhang, D.; Chen, Y.; Mei, K.; Chen, Q.; Wang, X.; Qiao, Z.; et al. Deep-Learning-Based Nanomechanical Vibration for Rapid and Label-Free Assay of Epithelial Mesenchymal Transition. *ACS Nano* **2024**, *18*, 3480–3496. [[CrossRef](#)] [[PubMed](#)]
124. Kadioğlu, H.G.; Civalak, Ö.; Uzun, B.; Yaylı, M.Ö. Size-dependent vibration and static analyses of a nanobeam made of time-dependent material attached with viscoelastic boundaries using three different beam theories. *Acta Mech.* **2025**, *236*, 1551–1578. [[CrossRef](#)]
125. Wang, P.; Xu, J.; Zhang, X.; Lv, Y. Free vibration of nanobeams with surface and dynamic flexoelectric effects. *Sci. Rep.* **2024**, *14*, 30192. [[CrossRef](#)] [[PubMed](#)]
126. Hoan, P.V.; Anh, N.D.; Thom, D.V.; Minh, P.V. Nonlinear vibration of nanobeams in thermal environment. *Mech. Based Des. Struct. Mach.* **2025**, *53*, 5690–5716. [[CrossRef](#)]
127. Mazari, M.Y.; Hamza, B.; Dehbi, F.; Cheikh, A.; Saimi, A.; Bensaid, I. Hybrid Galerkin-machine learning approach for dynamic analysis of nanocomposite beams under thermal effects. *Mech. Based Des. Struct. Mach.* **2025**, 1–18. [[CrossRef](#)]
128. Kenanda, M.A.; Hammadi, F.; Bahai, H.; Belabed, Z. A new efficient nonlocal hyperbolic HSDT for mechanical vibration of porous FGM plates/nanoplates using Navier's method and artificial neural network prediction. *Int. J. Solids Struct.* **2026**, *325*, 113719. [[CrossRef](#)]
129. Tariq, A.; Uzun, B.; Deliktaş, B.; Yaylı, M.Ö. Vibration analysis of embedded porous nanobeams under thermal effects using boosting machine learning algorithms and semi-analytical approach. *Mech. Adv. Mater. Struct.* **2024**, *31*, 12320–12343. [[CrossRef](#)]
130. Chen, X. Vibration behavior prediction of submerged nanobeams with axially traveling supports: Numerical, analytical, and machine learning approaches. *Mech. Based Des. Struct. Mach.* **2024**, *52*, 10273–10303. [[CrossRef](#)]
131. Tran, V.-T.; Nguyen, T.-K.; Nguyen-Xuan, H.; Abdel Wahab, M. Vibration and buckling optimization of functionally graded porous microplates using BCMO-ANN algorithm. *Thin-Walled Struct.* **2023**, *182*, 110267. [[CrossRef](#)]

132. Das, B.; Barretta, R.; Čanadija, M. Physics-Informed Neural Networks for Nonlocal Beam Eigenvalue Problems. *arXiv* **2025**, arXiv:2509.04321. [[CrossRef](#)]
133. Shakir, M.; Talha, M.; Dileep, A.D. Machine learning based probabilistic model for free vibration analysis of functionally graded graphene nanoplatelets reinforced porous plates. *Mech. Adv. Mater. Struct.* **2024**, *31*, 6095–6108. [[CrossRef](#)]
134. Siavashi, M.; Dardel, M.; Pashaei, M.H. Nonlinear stability and vibration analysis of fluid-conveying nanochannel scroll shells using an adaptive neuro-fuzzy inference system. *Thin-Walled Struct.* **2026**, *218*, 113931. [[CrossRef](#)]
135. Yan, G.; Zhou, X.; El-Meligy, M.A.; Sharaf, M. Nonlinear vibration analysis of graphene platelets reinforced nanocomposite doubly curved concrete panels subjected to thermal shock: Development of an artificial intelligence technique. *Mech. Adv. Mater. Struct.* **2024**, *31*, 7079–7100. [[CrossRef](#)]
136. Lin, Y.; Ibraheem, A.A. Machine learning method as a tool to estimate the vibrations of the concrete structures reinforced by advanced nanocomposites. *Mech. Adv. Mater. Struct.* **2025**, *32*, 777–793. [[CrossRef](#)]
137. Mazari, M.Y.; Hamza, B.; Slamene, A.; Dehbi, F.; Bensaid, I.; Mokhtari, M. Integrating machine learning with vibration analysis for graphene platelet nanocomposite beams subjected to magnetic loading. *Mech. Adv. Mater. Struct.* **2025**, 1–11. [[CrossRef](#)]
138. Belarbi, M.-O.; Khechai, A.; Bouhdjar, A.; Van Vinh, P.; Garg, A.; Li, L.; Garg, A. Assessment of free vibration frequencies of nano-scale functionally graded materials using hybrid machine learning approaches. *Neurocomputing* **2026**, *665*, 132194. [[CrossRef](#)]
139. Tariq, A.; Kadioğlu, H.G.; Uzun, B.; Deliktaş, B.; Yaylı, M.Ö. Modeling the viscoelastic behavior of a FG nonlocal beam with deformable boundaries based on hybrid machine learning and semi-analytical approaches. *Arch. Appl. Mech.* **2025**, *95*, 79. [[CrossRef](#)]

**Disclaimer/Publisher’s Note:** The statements, opinions and data contained in all publications are solely those of the individual author(s) and contributor(s) and not of MDPI and/or the editor(s). MDPI and/or the editor(s) disclaim responsibility for any injury to people or property resulting from any ideas, methods, instructions or products referred to in the content.